Angewandte Chemie
Eine Zeitschrift der Gesellschaft Deutscher Chemiker

Supporting Information

Cystine Knot Peptides with Tuneable Activity and Mechanism

C. Y. Li, F. B. H. Rehm, K. Yap, C. N. Zdenek, M. D. Harding, B. G. Fry, T. Durek, D. J. Craik, S. J. de Veer**

SUPPORTING INFORMATION

Cystine Knot Peptides with Tuneable Activity and Mechanism

Choi Yi Li[+], Fabian B. H. Rehm[+], Kuok Yap, Christina N. Zdenek, Maxim D. Harding, Bryan G. Fry, Thomas Durek, David J. Craik*, Simon J. de Veer*

C. Y. Li,[+] F. B. H. Rehm,[+] K. Yap, M. D. Harding, T. Durek, D. J. Craik, S. J. de Veer

Institute for Molecular Bioscience, Australian Research Council Centre of Excellence for Innovations in Peptide and Protein Science, The University of Queensland, Brisbane, QLD 4072 (Australia)

*Email: s.deveer@imb.uq.edu.au and d.craik@imb.uq.edu.au

C. N. Zdenek, B. G. Fry

Venom Evolution Lab, School of Biological Sciences, The University of Queensland, Brisbane, QLD 4072 (Australia)

[+] These authors contributed equally to this work

Experimental Section

Reagents

Fmoc Nα-protected amino acids were from CSBio, except for Fmoc-L-norleucine, Fmoc-L-Lys(biotin), Fmoc-4-azido-L-Phe, Fmoc-4-fluoro-L-Phe, Fmoc-4-methyl-L-Phe, and Fmoc-L-homo-Glu(OtBu), which were from Chem-Impex. Solvents for peptide synthesis (N,N-dimethylformamide [DMF] and dichloromethane [DCM]) were from Chem-Supply, N,N-diisopropylethylamine (DIPEA) was from Merck, and O-(1H-6-chlorobenzotriazole-1-yl)-1,1,3,3-tetramethyluronium hexafluorophosphate (HCTU) or benzotriazol-1-yloxy-tripyrrolidino-phosphonium hexafluorophosphate (PyBOP) for amino acid coupling were from CSBio or Mimotopes, respectively. Acetonitrile for reverse-phase high-performance liquid chromatography (HPLC) was from Merck. Human proteases purified from plasma or tissue were sourced from Sigma-Aldrich (cationic trypsin, plasmin) or Molecular Innovation (coagulation β-factor XIIa, coagulation factor XIa, coagulation factor Xa, α-thrombin, plasma kallikrein). Recombinant human matriptase (catalytic domain) was obtained from R&D Systems, and recombinant KLK4, tPA, and uPA were expressed in Sf9 insect cells[1] or Expi293 cells[2] as previously described. Commercially available synthetic peptide-MCA substrates were from Peptide Institute, except Boc-VPR-MCA (Bachem). Streptavidin was obtained as a 1 mg mL^{-1} solution (New England Biolabs) or lyophilised 1 mg units (Promega).

Peptide synthesis

Knottin PI variants were assembled by automated Fmoc solid-phase synthesis on 2-chlorotrityl chloride resin (0.45 mmol g^{-1}, CSBio) using a Symphony multiplex peptide synthesiser (Protein Technologies). Coupling reactions (2 × 10 min) were performed using 4 eq. amino acid dissolved in DMF with 4 eq. HCTU and 8 eq. DIPEA. Deprotection of the N-terminal Fmoc protecting group was performed using 30% piperidine (2 × 3 min). Once assembled, peptides were cleaved from the resin and side chains deprotected using trifluoroacetic acid (TFA)/triisopropylsilane/H_2O (96:2:2) at room temperature (3 h). The resin was removed by filtration, and peptides were precipitated in ice-cold diethyl ether. Recovered material was dissolved in water/acetonitrile (4:1) and lyophilised. Crude peptides were purified by reverse-phase HPLC using a Phenomenex Jupiter C18 column (5 μm 300 Å, 250 × 21.2 mm) and a linear gradient of 5–45% acetonitrile in H_2O containing 0.05%

TFA. Fractions were analysed by electrospray ionisation mass spectrometry (Shimadzu Prominence) to identify those containing the desired product. These fractions were pooled and diluted in 0.1 M ammonium bicarbonate (pH 8.3) for oxidative folding (room temperature, stirring, 24 h) to allow formation of the cystine knot. Folded knottins were isolated via a second reverse-phase HPLC purification step and validated by mass spectrometry (as above). Peptide purity was assessed by UHPLC (Shimadzu Nexera) using a Phenomenex Luna Omega C18 column (1.6 µm 100 Å, 50 × 2.1 mm) or analytical HPLC (Shimadzu Nexera XR) using a Phenomenex Jupiter C18 column (5 µm 300 Å, 150 × 2 mm).

NMR spectroscopy

Peptides were dissolved in H_2O/D_2O (10:1) at a concentration of ~1 mg/mL and adjusted to pH 3–4. ^{1}H one-dimensional (1D), total correlation spectroscopy (TOCSY), and nuclear Overhauser effect spectroscopy (NOESY) experiments were performed at 298 K using a Bruker Avance III 600 MHz spectrometer equipped with a cryogenically cooled probe. Mixing times were 80 ms (TOCSY) and 200 ms (NOESY). Spectra from TOCSY or NOESY experiments were referenced to DSS (0.00 ppm).

Chemoenzymatic synthesis

A head-to-tail cyclic knottin based on the FXIIa-selective inhibitor **1** was produced by chemoenzymatic synthesis. The linear precursor (sequence: GGVCPR^{4F}FEKKCRRDSDCPGACICRGNGYCGSGSDAL, ^{4F}F = 4-fluoro-L-Phe) was assembled by automated Fmoc solid-phase synthesis (Symphony), deprotected, folded, and purified as described above for acyclic knottins. The native cyclase from *Momordica cochinchinensis*, MCoAEP2,[3] was used to cyclise this precursor at the C-terminal recognition site (D↓AL). The reaction was run under the same conditions as cyclisation of MCoTI-II by MCoAEP2, as described previously.[4] Recombinant MCoAEP2 was expressed in *E. coli*, then purified and activated as described previously.[4]

Native chemical ligation

A peptide hydrazide[5] (sequence: RVCPR^{4F}FEKB-NHNH$_2$, ^{4F}F = 4-fluoro-L-Phe, B = Nε-biotinyl-L-Lys) was synthesised on 2-chlorotrityl resin that had been derivatised with 5% hydrazine in DMF (3 × 30 min). The first amino acid (4 eq.) was manually coupled using 4 eq. PyBOP and 4 eq. DIPEA (2 × 30 min), and all subsequent

deprotection and coupling reactions were carried out by automated peptide synthesis (Symphony), as described earlier. The C-terminal knottin fragment (sequence: CRRDSDCPGACICRGNGYCG) was produced by automated peptide synthesis. Assembled peptides were cleaved from the resin and side chains deprotected using TFA/triisopropylsilane/H_2O (96:2:2) at room temperature (3 h), and purified by reverse-phase HPLC.

The peptide hydrazide was converted to a thioester under mild conditions using the method described by Dawson and colleagues.[6] Briefly, 5.04 mg peptide hydrazide was dissolved in 6 M guanidine hydrochloride pH 3 (peptide concentration: 4 mM), to which 2 equiv. acetylacetone (Sigma-Aldrich) was added. This solution was added to 4-mercaptophenylacetic acid (Sigma-Aldrich, final concentration: 200 mM), and incubated for 4 h (room temperature, gentle stirring). The C-terminal fragment (8.21 mg, 1.1 equiv.) was dissolved in 0.2 M sodium phosphate buffer pH 7.2 containing 6 M guanidine hydrochloride and 50 mM tris(2-carboxyethyl)phosphine (peptide concentration: 5 mM), then added to thioesterification reaction. The pH was adjusted to 7 and the ligation reaction (final volume: 1.7 mL) was left to proceed overnight (room temperature, gentle stirring). The crude ligation products were diluted 1:50 in 0.1 M ammonium bicarbonate pH 8.3 containing 3 mM GSSG, and incubated for 24 h (stirring) to allow formation of the cystine knot. After lowering the pH to 3, the desired product **1** was isolated following a single reverse-phase HPLC purification (5.2 mg, 42% isolated yield based on the starting amount of peptide hydrazide).

Protease inhibition assays

Knottin variants in each positional library were screened at a fixed concentration for each protease (trypsin: 10 nM, FXIIa: 25 nM, matriptase: 5 nM, KLK4: 1.25 nM) in competitive inhibition assays. Briefly, inhibitors were diluted in 96-well assay plates (Corning) in buffer (0.1 M Tris-HCl pH 8, 0.1 M NaCl, 0.005% Triton X-100, buffer also included 10 mM $CaCl_2$ for trypsin and FXIIa) before adding a fixed concentration of protease. After incubating the plates to allow each protease/inhibitor system to reach equilibrium, a fixed concentration of substrate was added and enzyme activity was measured using a TECAN M1000 infinite plate reader. Specific conditions for each protease are listed in the table below (page S5). Assays using a peptide 4-methylcoumaryl-7-amide (peptide-MCA) substrate were performed in black 96-well plates, with cleavage of the MCA moiety monitored for 10 min (λ_{ex} = 360 nm, λ_{em} = 460 nm, reading interval: 60 s). Assays using a peptide *para*-nitroanilide (peptide-pNA) substrate were performed in transparent 96-well plates, with cleavage

of the pNA moiety monitored for 10 min (λ_{abs} = 405 nm, reading interval: 30 s). For each knottin variant, the percentage inhibition was calculated by comparing the rate with inhibitor (RFU min^{-1} or mOD min^{-1}) to control wells with protease and substrate only. Three experiments were performed in duplicate. Assays to determine the inhibition constant (K_i) were performed using a similar method, except that a serial dilution of inhibitor was tested. Data from three experiments performed in triplicate were analysed in GraphPad Prism 9 to determine K_i by non-linear regression (Morrison equation).

Protease	Protease Conc. (nM)	Substrate	Substrate Conc. (μM)	K_M (μM)[#]
Factor XIIa*	6	Ac-QRFR-pNA	120	160
Trypsin*	0.1	Boc-VPR-MCA	5	3.7
Matriptase	0.6	Boc-QAR-MCA	10	42
KLK4	0.75	Boc-VPR-MCA	50	13
Thrombin*	0.1	Boc-VPR-MCA	40	-
FXa*	0.2	Z-Pyr-GR-MCA	50	-
FXIa*	1	Boc-Glu(OBzl)-AR-MCA	100	-
Plasmin	1	Ac-RM(O_2)YR-pNA	75	-
Plasma kallikrein	0.5	Z-FR-MCA	50	-
uPA*	10	Z-Pyr-GR-MCA	100	-
tPA*	10	Z-Pyr-GR-MCA	100	-

*Buffer for these enzymes included 10 mM $CaCl_2$
[#]K_M values are listed for enzymes where K_i values are reported in the manuscript

Assays to study inhibitor dissociation rates were performed using a previously described method.[7] These experiments monitor substrate cleavage under three conditions: substrate added to enzyme simultaneously with inhibitor, substrate added to enzyme pre-incubated with inhibitor, and substrate added to enzyme without inhibitor (control). Chromogenic substrates were used for both enzymes to allow activity to be monitored using an absolute measure (A405 nm). Assays for FXIIa used 6 nM enzyme, 150 μM Ac-QRFR-pNA and 15 nM **MCoLib** or 30 nM compound **1**. Assays for trypsin used 0.5 nM enzyme, 150 μM Ac-YASR-pNA and 2.5 nM **MCoLib** or 10 μM compound **1**. Substrate cleavage was monitored using a TECAN M1000 infinite plate reader (λ_{abs} = 405 nm, reading interval: 30 s). Progress curves were generated by plotting the change in absorbance (mOD) over time, which allow calculation of k_{off} using the formula: $k_{off} = (|\tau| + |\tau^*|)^{-1}$ where τ and τ^* represent the *x*-intercept of the reaction curve at steady state from simultaneous addition of substrate and inhibitor or pre-incubated enzyme and inhibitor. Experiments were performed three times in triplicate.

Ethics statement

Surplus citrated human plasma from healthy adults was sourced from a national repository (The Australian Red Cross) under Research Agreement #18-03QLD-09, The University of Queensland Human Ethics Committee Approval #2016000256, and The University of Queensland Biosafety Committee Approval #IBC134BSBS2015. Frozen plasma was defrosted, aliquoted, flash-frozen, and stored at −80°C, according to previously established protocols.[8]

Coagulation assays

Two coagulation assays were used to study inhibitor effects on the clotting time of human plasma. The activated partial thromboplastin time (aPTT) assay uses a kaolin reagent (clay) to activate the intrinsic pathway of the coagulation cascade, and the prothrombin time (PT) assay uses Neoplastine (lyophilised rabbit thromboplastin) to activate the extrinsic pathway. A minor adjustment to the manufacturer's standard protocol was made to both tests (addition of 25 µL inhibitor or buffer, see table below) to accommodate the addition of inhibitor without changing the total volume (and thus, ratios of additives) of the assay, as described previously.[9] Concentrations of inhibitor are reported as the concentration at the point of incubation in the assay, i.e. not taking into account the addition of the start reagent (calcium for aPTT, or Neoplastine for PT) – this approach reflects the inhibitor concentration in the initial plasma sample.

Experiment	Methodology
aPTT	Step 1: 50 µL human plasma + 25 µL inhibitor* (solubilised in Owren–Koller (OK) Buffer (isotonic saline, Stago # 00360)) + 50 µL kaolin/phospholipid (Stago # 00597) Step 2: 240 s incubation at 37°C Step 3: Addition of 50 µL 0.025 M calcium (Stago # 00367)
PT	Step 1: 50 µL human plasma + 25 µL inhibitor* (diluted with OK Buffer) Step 2: 240 s incubation at 37°C Step 3: Addition of 100 µL Neoplastine (Stago #00606)

*Control assays replaced 25 µL inhibitor with 25 µL OK buffer.
aPTT = Activated Partial Thromboplastin Time, PT = Prothrombin Time.

Plasma clotting time (s) was automatically measured using a STA-R Max® analyser (Stago, Asnières sur Seine, France). Measurements were conducted using a viscosity-based (mechanical) detection system where

opposing magnets oscillate a small metal spherical pellet inside the test cuvette until a clot is formed. Dilution of the inhibitor in Owren–Koller (OK) buffer for dose-response curves was performed automatically by the machine. Reagents were kept at 15–19 °C in the machine during experimentation and otherwise stored at 4 °C. All tests were performed in triplicate.

UV crosslinking assays

All crosslinking experiments were performed in glass screwcap vials (32 × 12 mm, Agilent Technologies) using a standard transilluminator (Biorad GelDoc XR+) as the UV light source (λ = 302 nm). Briefly, protease–knottin samples were mixed and incubated for 10 min at room temperature, then added to a glass vial (final volume: 100 µL). Vials were placed on the transilluminator and exposed to UV light for 0.5–5 min. Samples for enzyme kinetic assays were prepared using 8 × assay final concentration of protease and a serial dilution of inhibitor. Samples for SDS-PAGE or mass spectrometry analyses were prepared using 5 µM FXIIa and 10 µM knottin (**1X1** or **1X2**). For additional controls where FXIIa was pre-incubated with a high-affinity competing inhibitor, 5 µM FXIIa was incubated with 5 µM or 10 µM compound **7** (Table S6) for 10 min prior to adding the photoactive knottin.

For kinetic assays, 25 µL of sample was added to duplicate wells of a 96-well plate containing 125 µL assay buffer. Immediately prior to assay, a fixed concentration of substrate was added (volume added: 50 µL), such that the final volume was 200 µL. Final concentrations of protease and substrate were as shown on page S5. Enzyme activity was measured using a TECAN M1000 infinite plate reader, as described above (protease inhibition assays). Data for each UV exposure time are expressed as % inhibition relative to controls (protease only) that had been exposed to UV light for the same time. Experiments were performed using three independently prepared UV-exposed samples and were assayed in duplicate. For SDS-PAGE analysis, samples were diluted in loading buffer (Bolt™ LDS sample buffer, Novex) and boiled at 95°C for 5 min. Samples were run on 4–12% gradient gels (Bolt™ 4–12% Bis-Tris Plus) using MES SDS running buffer (Novex). Gels were stained with InstantBlue™ Coomassie Protein Stain (Expedeon). For mass spectrometry, FXIIa or the FXIIa-**1X2** complex were loaded onto a Zorbax 300SB-C18 column (Agilent) and eluted over an 8 min 1–80% acetonitrile gradient. The liquid chromatography outflow was connected to a 5600 Triple TOF mass spectrometer (SCIEX) (Turbo V ion source). Reconstructed spectra were generated using MagTran (Amgen).

Activity assays with streptavidin

The effect of streptavidin on the inhibitory activity of biotinylated knottins was initially examined in competitive inhibition assays. In 96-well plates, FXIIa (12 nM) was incubated with **1B** (250 nM) for 10 min (volume: 100 µL – note that final assay concentrations were 6 nM FXIIa and 125 nM **1B**). Next, varying concentrations of streptavidin (0.25–1 equiv. relative to **1B**) or an equivalent volume of buffer (50 µL) were added. After 10 min incubation, 50 µL substrate was added (120 µM) and FXIIa activity was monitored using a TECAN M1000 infinite plate reader (λ_{abs} = 405 nm, 30 s reading interval). Controls with FXIIa, the non-labelled inhibitor (**1**) and 1 equiv. streptavidin, or FXIIa ± streptavidin (without inhibitor) were also included. This assay setup was also used to switch OFF **LibB** with FXIIa, trypsin, matriptase, and KLK4. Specific conditions (final assays concentrations) were: FXIIa (6 nM) with 120 µM Ac-QRFR-pNA and 50 nM **LibB** or **MCoLib**; trypsin (0.1 nM) with 5 µM Boc-VPR-MCA and 10 nM **LibB** or **MCoLib**; matriptase (0.6 nM) with 10 µM Boc-QAR-MCA and 5 nM **LibB** or **MCoLib**; or KLK4 (0.75 nM) with 50 µM Boc-VPR-MCA and 2.5 nM **LibB** or **MCoLib**. All assays were performed three times in triplicate.

To examine how quickly streptavidin can switch OFF biotinylated knottins, additional experiments were performed where substrate was added immediately after the addition of streptavidin. In these assays, FXIIa (12 nM) was incubated with **1B** (250 nM) for 10 min (volume: 100 µL – final concentrations were FXIIa: 6 nM; **1B**: 125 nM). Next, 0.25–1 equiv. streptavidin (relative to **1B**) or an equivalent volume of buffer (50 µL) was added, followed by immediate addition of substrate (120 µM). FXIIa activity was monitored as described above, and assays were performed three times in triplicate.

We also explored whether a biotinylated knottin and streptavidin could be used to stop then restart an enzymatic reaction in progress. Here, reactions were initiated by adding FXIIa (5 nM) to substrate (150 µM), volume = 190 µL, and activity was monitored at λ_{abs} = 405 nm. After 5 min, the plate was ejected and **1B** (500 nM) was added to stop the reaction by adding 5 µL from a 20 µM stock solution. After a further 5 min, the plate was ejected and streptavidin (500 nM, 5 µL from a 20 µM stock solution) or an equivalent volume of buffer was added. FXIIa activity was monitored for a further 8 min. After each addition, well contents were mixed manually with a multichannel pipette. Controls were also included where FXIIa was added to substrate, but **1B** or streptavidin were not added. Additional experiments were performed to test whether a second stop-

start cycle was possible. Reactions were initiated by adding FXIIa (5 nM) to substrate (150 μM), then adding 500 nM **1B** after 5 min, followed by 500 nM streptavidin after a further 5 min, as described above. After a further 7 min, the plate was ejected and 2000 nM **1B** (5 μL from an 80 μM stock solution) was added. After a further 5 min, the plate was ejected and 2000 nM streptavidin (5 μL from an 80 μM stock solution) was added. FXIIa activity was monitored for a further 7 min. All assays were performed three times in triplicate.

The effect of crosslinking the inhibitor and enzyme on the ability of streptavidin to switch OFF inhibitory activity was assessed using a biotinylated analogue of **1X2** (named **1X2B**). Initially, crosslinking assays were performed with FXIIa and trypsin (kinetic assays as described on page S7) to confirm that **1X2B** retained similar inhibitory activity to its non-labelled counterpart. Subsequently, crosslinked enzyme–**1X2B** complexes were prepared for incubation with streptavidin prior to adding substrate. These samples were prepared by incubating 48 nM FXIIa with 500 nM **1X2B** or 0.8 nM trypsin with 8 μM **1X2B** (all reagents 8 × final assay concentration, 100 μL volume) for 10 min, followed by exposure to UV light for 3 min (FXIIa) or 5 min (trypsin). From each vial, 25 μL of enzyme + **1X2B** was added to wells containing 75 μL buffer (in triplicate). Next, varying concentrations of streptavidin (0.25–1 equiv. relative to **1X2B**) or an equivalent volume of buffer (50 μL) were added, and the plate was incubated for 10 min. After adding substrate (50 μL, 120 μM Ac-QRFR-pNA [FXIIa] or 5 μM Boc-VPR-MCA [trypsin]), enzyme activity was monitored as described above.

To test whether a biotinylated knottin can be switched OFF in human plasma, we modified the coagulation (aPTT) assay described earlier (page S6) to include a second incubation with streptavidin or buffer (control). The first incubation was carried on in a 37°C heating block (240 s) with 1 mL samples (ratio 2:1:2 for plasma, inhibitor/buffer and kaolin + phospholipid). This material was transferred to a STA-R Max® analyser, which dispensed 125 μL sample per test cuvette, followed by 25 μL streptavidin (0.5 or 1 equiv. relative to inhibitor) or OK buffer. Cuvettes were incubated at 37°C for 240 s, followed by addition of $CaCl_2$ and measurement of clotting time using automated functions on the analyser, as described earlier. Modifications to the assay protocol are shown on page S10.

Experiment	Methodology
aPTT	Step 1: 50 µL human plasma + 25 µL inhibitor* (solubilised in Owren–Koller (OK) Buffer (isotonic saline) + 50 µL kaolin/phospholipid Step 2: 240 s incubation at 37°C Step 3: Transfer material to analyser and dispense 125 µL per test cuvette Step 4: Addition of 25 µL streptavidin* Step 5: 240 s incubation at 37°C Step 6: Addition of 50 µL 0.025 M calcium

*Control assays replaced 25 µL inhibitor and/or 25 µL streptavidin with 25 µL OK buffer

Supplementary Results 1

Producing separate MCoTI-II libraries with the full complement of proteinogenic amino acids at four positions requires 80 cyclic peptides. Therefore, we considered two strategies to simplify library synthesis. First, the number of amino acids included at each position was decreased to ten (methionine was replaced by an isostere, norleucine) to halve the number of peptides whilst still maintaining chemical diversity in the library. Second, an acyclic variant was designed by replacing the eight-residue loop 6 of MCoTI-II with the N- and C-terminal residues from the closely-related acyclic knottin MCoTI-V.[10] Aligned sequences are shown below:

This change includes an N-terminal Arg residue that is found in many acyclic knottins[11] and forms an intramolecular salt-bridge with the C-terminal carboxyl that, in effect, leads to pseudo-cyclisation.[12, 13] Incorporating these modifications into MCoTI-II did not lead to structural changes in other loops, as seen by ^{1}H NMR experiments where the acyclic and cyclic MCoTI-II variants had similar secondary Hα chemical shifts (Figure S1). The acyclic template, named **MCoLib**, was generated after one final change (replacing the P1 Lys residue with Arg, as seen in MCoTI-V).

Figure S1

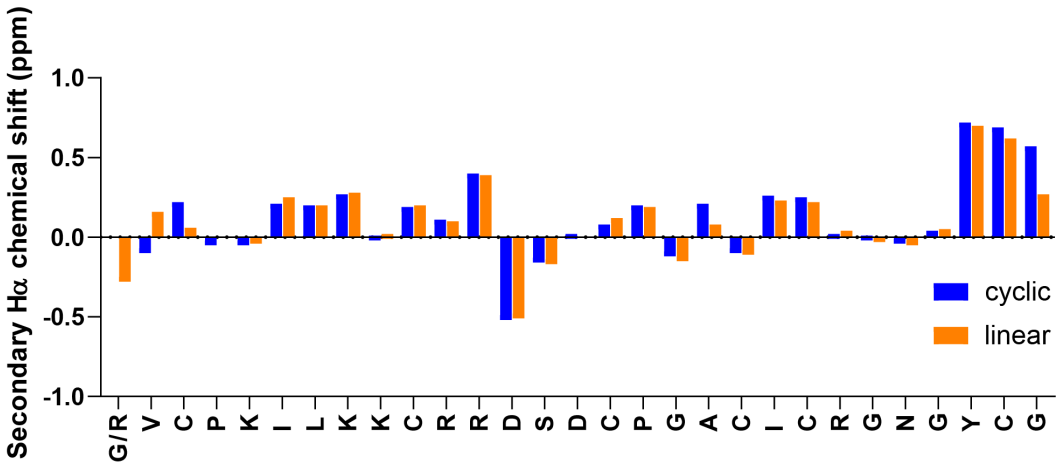

Figure S1. Secondary Hα chemical shifts for cyclic MCoTI-II and an acyclic variant. Spectra were referenced to 2,2-dimethyl-2-silapentane-5-sulfonic acid at 0.00 ppm, and secondary Hα chemical shifts were calculated by subtracting the random coil chemical shift[14] from the observed shift, as described previously.[9]

The knottin variants in each positional library were synthesised by automated Fmoc solid-phase peptide synthesis, then purified by reverse-phase HPLC prior to oxidative folding to form the cystine knot. After purification of the folded knottins, peptides were analysed by LC/MS and ^{1}H 1D NMR spectroscopy (Figure S2–S9, Table S1–S4) to confirm that each knottin was pure and had a well-defined conformation. The latter analyses revealed that each peptide produced ^{1}H 1D spectra with sharp, well-dispersed peaks in the amide spectral region (7–9 ppm), indicating that substituting diverse amino acids at the P1′–P4′ positions did not impair the well-defined structure of the knottin scaffold.

Figure S2

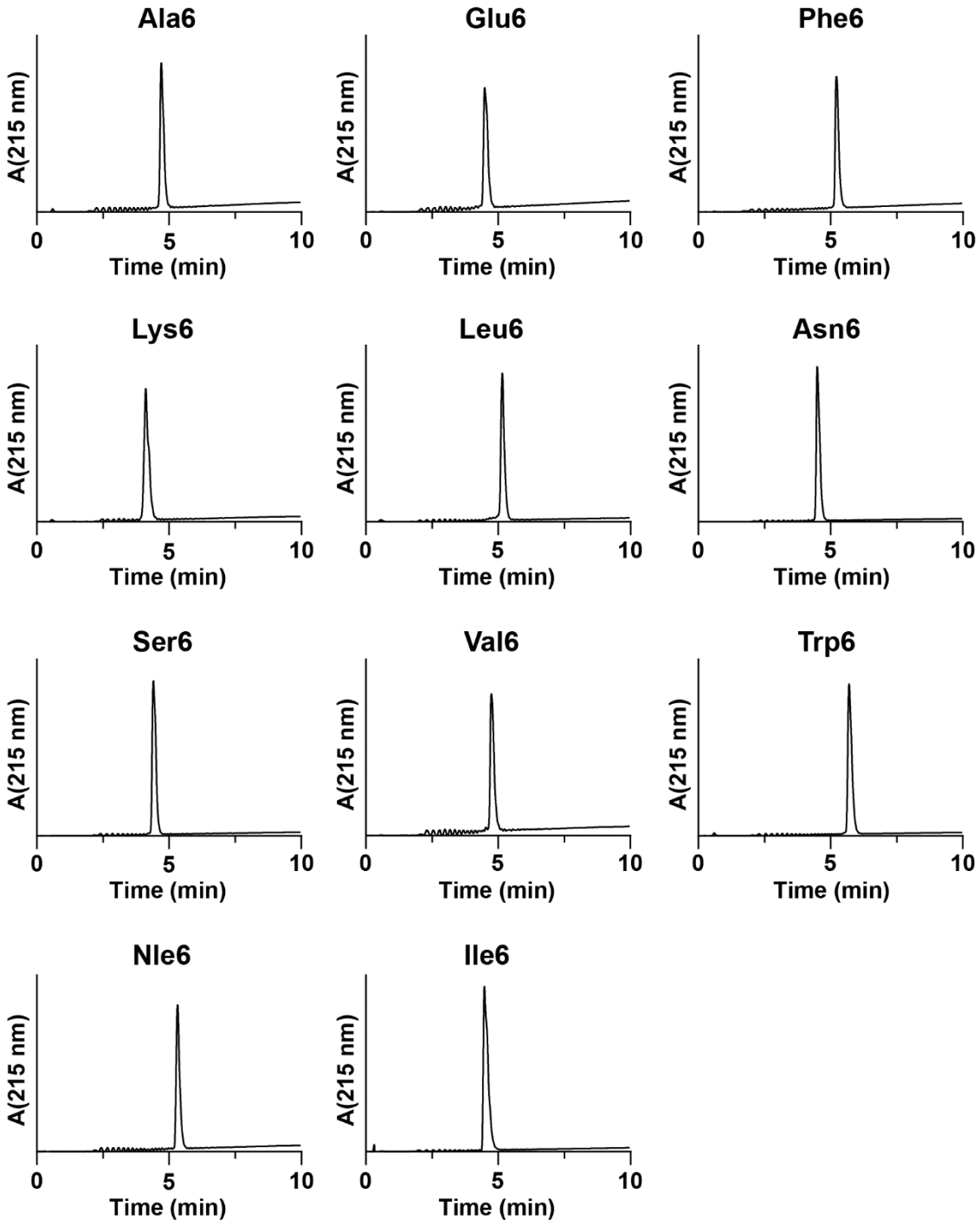

Figure S2. Analytical UHPLC traces for knottin variants with amino acid substitutions at P1′. Data were acquired using a Shimazdu Nexera UHPLC system equipped with a Phenomenex Luna Omega C18 column (1.6 µm 100 Å, 50 × 2.1 mm). Peptide sequences are listed in Table S1 (page S14). Ile6 is also referred to as **MCoLib**. Nle denotes norleucine.

Table S1

Comp.	Sequence[a]	Theoretical $[M+3H]^{3+}$	Observed $[M+3H]^{3+}$	Purity (%)
Ala6	RVCPR**A**LKKCRRDSDCPGACICRGNGYCG	1051.9	1051.8	>99
Glu6	RVCPR**E**LKKCRRDSDCPGACICRGNGYCG	1071.3	1071.2	>99
Phe6	RVCPR**F**LKKCRRDSDCPGACICRGNGYCG	1077.3	1077.2	>99
Lys6	RVCPR**K**LKKCRRDSDCPGACICRGNGYCG	1070.9	1070.8	>99
Leu6	RVCPR**L**LKKCRRDSDCPGACICRGNGYCG	1065.9	1065.8	>99
Asn6	RVCPR**N**LKKCRRDSDCPGACICRGNGYCG	1066.2	1066.1	>99
Ser6	RVCPR**S**LKKCRRDSDCPGACICRGNGYCG	1057.2	1057.0	>99
Val6	RVCPR**V**LKKCRRDSDCPGACICRGNGYCG	1061.3	1061.1	>99
Trp6	RVCPR**W**LKKCRRDSDCPGACICRGNGYCG	1090.3	1090.1	>99
Nle6	RVCPR**Nle**LKKCRRDSDCPGACICRGNGYCG	1065.9	1065.7	>99
Ile6	RVCPR**I**LKKCRRDSDCPGACICRGNGYCG	1065.9	1065.8	>99

[a]Residue substitutions are shown in red bold font. Ile6 is also referred to as MCoLib. Nle = norleucine

Figure S3

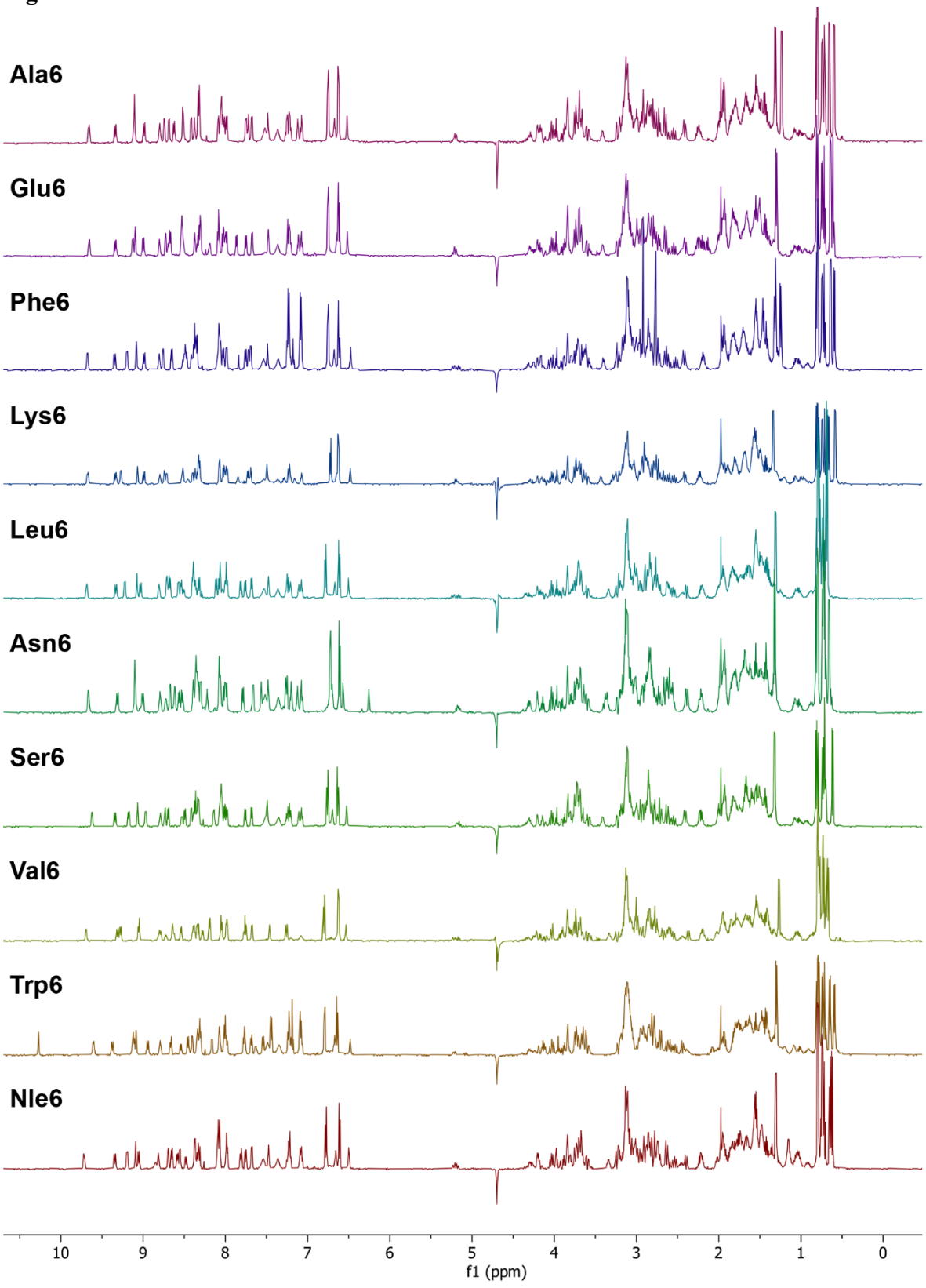

Figure S3. ^{1}H 1D NMR spectra for knottin variants with amino acid substitutions at P1′. Peptide sequences are listed in Table S1 (page S14).

Figure S4

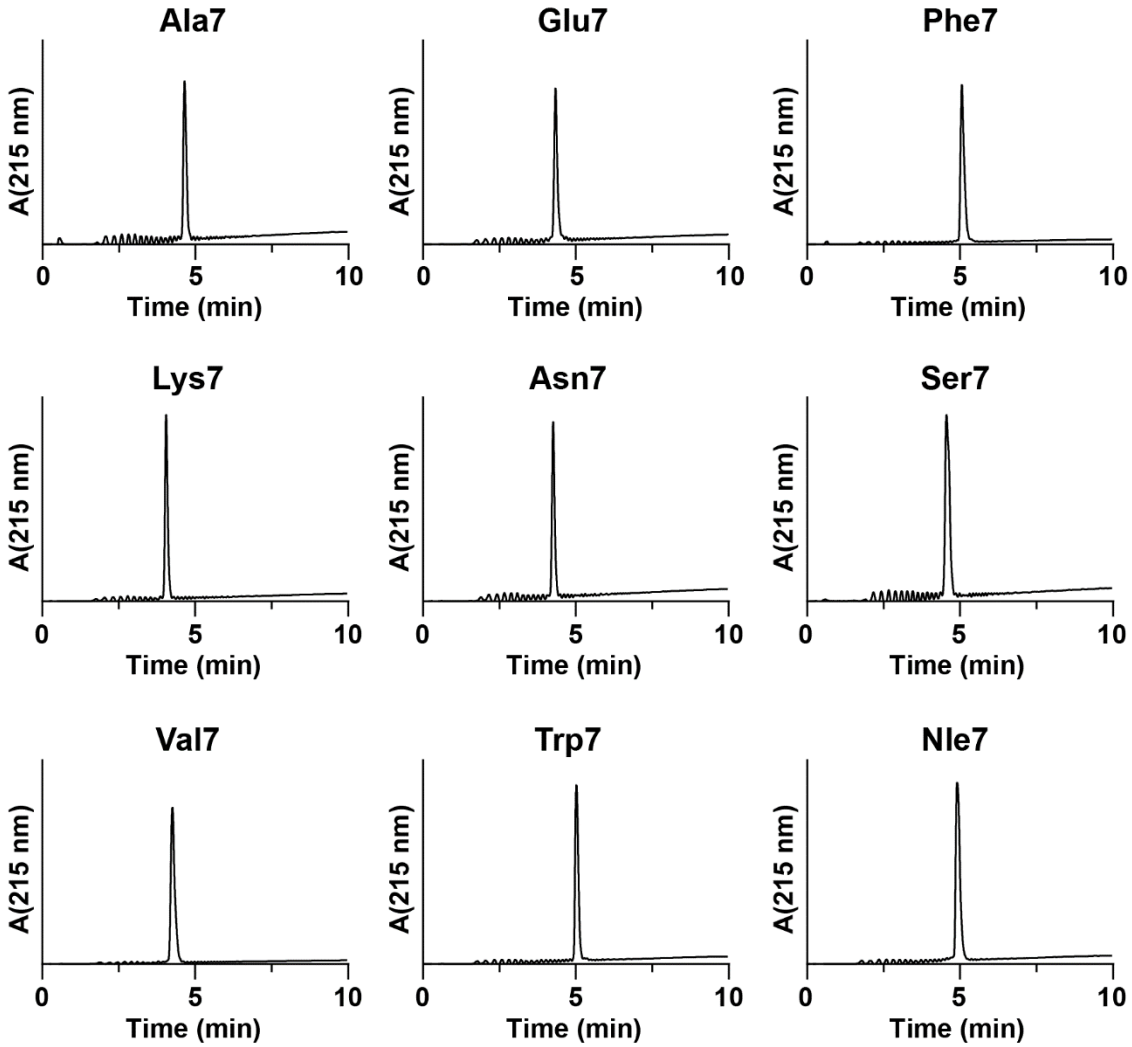

Figure S4. Analytical UHPLC traces for knottin variants with amino acid substitutions at P2′. Data were acquired using a Shimazdu Nexera UHPLC system equipped with a Phenomenex Luna Omega C18 column (1.6 µm 100 Å, 50 × 2.1 mm). Peptide sequences are listed in Table S2 (page S17). Nle denotes norleucine.

Table S2

Comp.	Sequence[a]	Theoretical $[M+3H]^{3+}$	Observed $[M+3H]^{3+}$	Purity (%)
Ala7	RVCPRI**A**KKCRRDSDCPGACICRGNGYCG	1051.9	1051.8	>99
Glu7	RVCPRI**E**KKCRRDSDCPGACICRGNGYCG	1071.3	1071.3	>99
Phe7	RVCPRI**F**KKCRRDSDCPGACICRGNGYCG	1077.3	1077.2	>99
Lys7	RVCPRI**K**KKCRRDSDCPGACICRGNGYCG	1070.9	1070.8	>99
Asn7	RVCPRI**N**KKCRRDSDCPGACICRGNGYCG	1066.2	1066.2	>99
Ser7	RVCPRI**S**KKCRRDSDCPGACICRGNGYCG	1057.2	1057.0	>99
Val7	RVCPRI**V**KKCRRDSDCPGACICRGNGYCG	1061.3	1061.2	>99
Trp7	RVCPRI**W**KKCRRDSDCPGACICRGNGYCG	1090.3	1090.2	>99
Nle7	RVCPRI**Nle**KKCRRDSDCPGACICRGNGYCG	1065.9	1065.8	>99

[a]Residue substitutions are shown in red bold font. Nle = norleucine

Figure S5

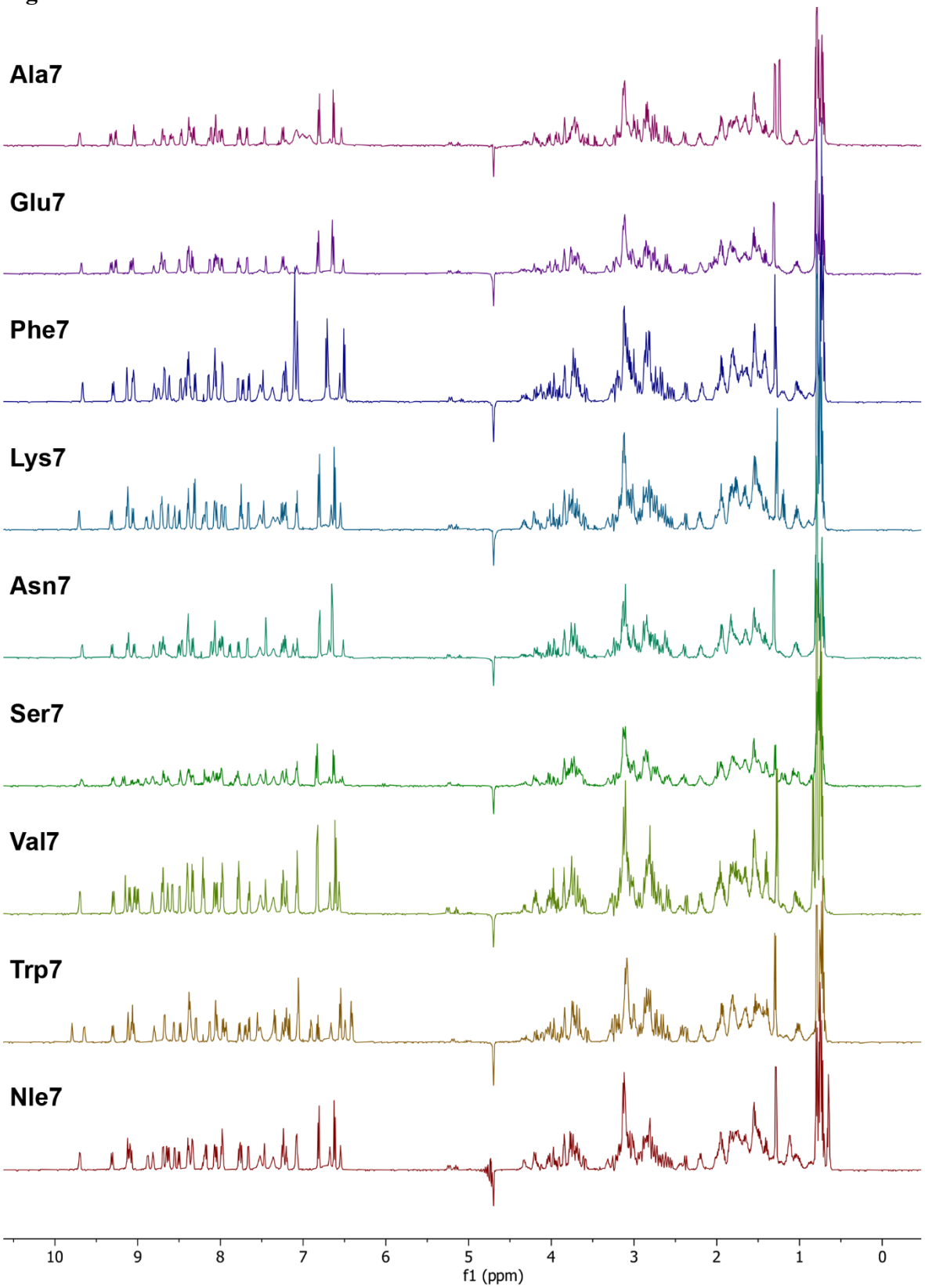

Figure S5. ^{1}H 1D NMR spectra for knottin variants with amino acid substitutions at P2′. Peptide sequences are listed in Table S2 (page S17).

Figure S6

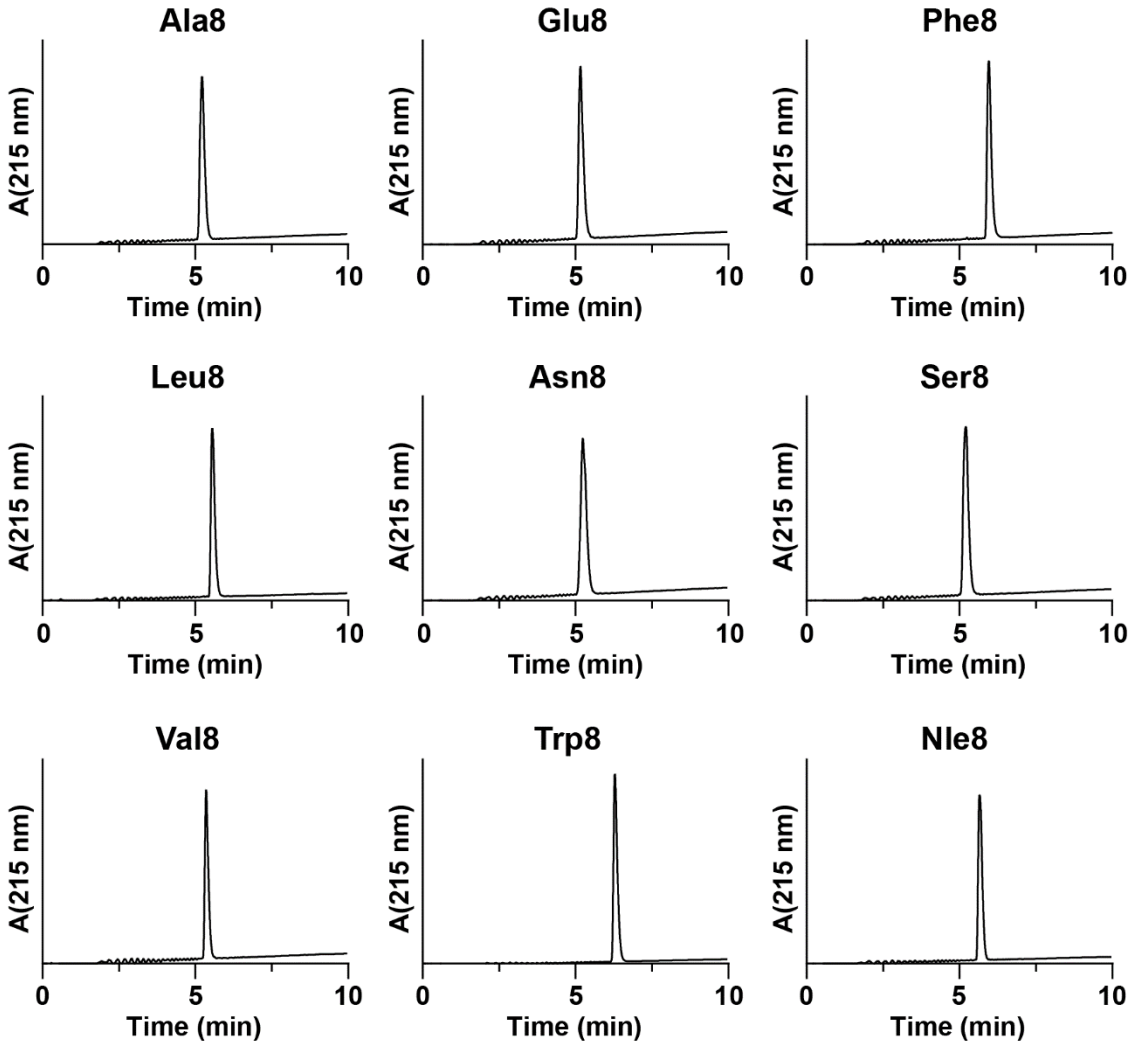

Figure S7. Analytical UHPLC traces for knottin variants with amino acid substitutions at P3′. Data were acquired using a Shimazdu Nexera UHPLC system equipped with a Phenomenex Luna Omega C18 column (1.6 µm 100 Å, 50 × 2.1 mm). Peptide sequences are listed in Table S3 (page S20). Nle denotes norleucine.

Table S3

Comp.	Sequence[a]	Theoretical $[M+3H]^{3+}$	Observed $[M+3H]^{3+}$	Purity (%)
Ala8	RVCPRIL**A**KCRRDSDCPGACICRGNGYCG	1046.9	1046.8	>99
Glu8	RVCPRIL**E**KCRRDSDCPGACICRGNGYCG	1066.2	1066.2	>99
Phe8	RVCPRIL**F**KCRRDSDCPGACICRGNGYCG	1072.3	1072.2	>99
Leu8	RVCPRIL**L**KCRRDSDCPGACICRGNGYCG	1060.9	1060.8	>99
Asn8	RVCPRIL**N**KCRRDSDCPGACICRGNGYCG	1061.2	1061.1	>99
Ser8	RVCPRIL**S**KCRRDSDCPGACICRGNGYCG	1052.2	1052.2	>99
Val8	RVCPRIL**V**KCRRDSDCPGACICRGNGYCG	1056.3	1056.2	>99
Trp8	RVCPRIL**W**KCRRDSDCPGACICRGNGYCG	1085.3	1085.2	>99
Nle8	RVCPRIL**Nle**KCRRDSDCPGACICRGNGYCG	1060.9	1060.9	>99

[a]Residue substitutions are shown in red bold font. Nle = norleucine

Figure S7

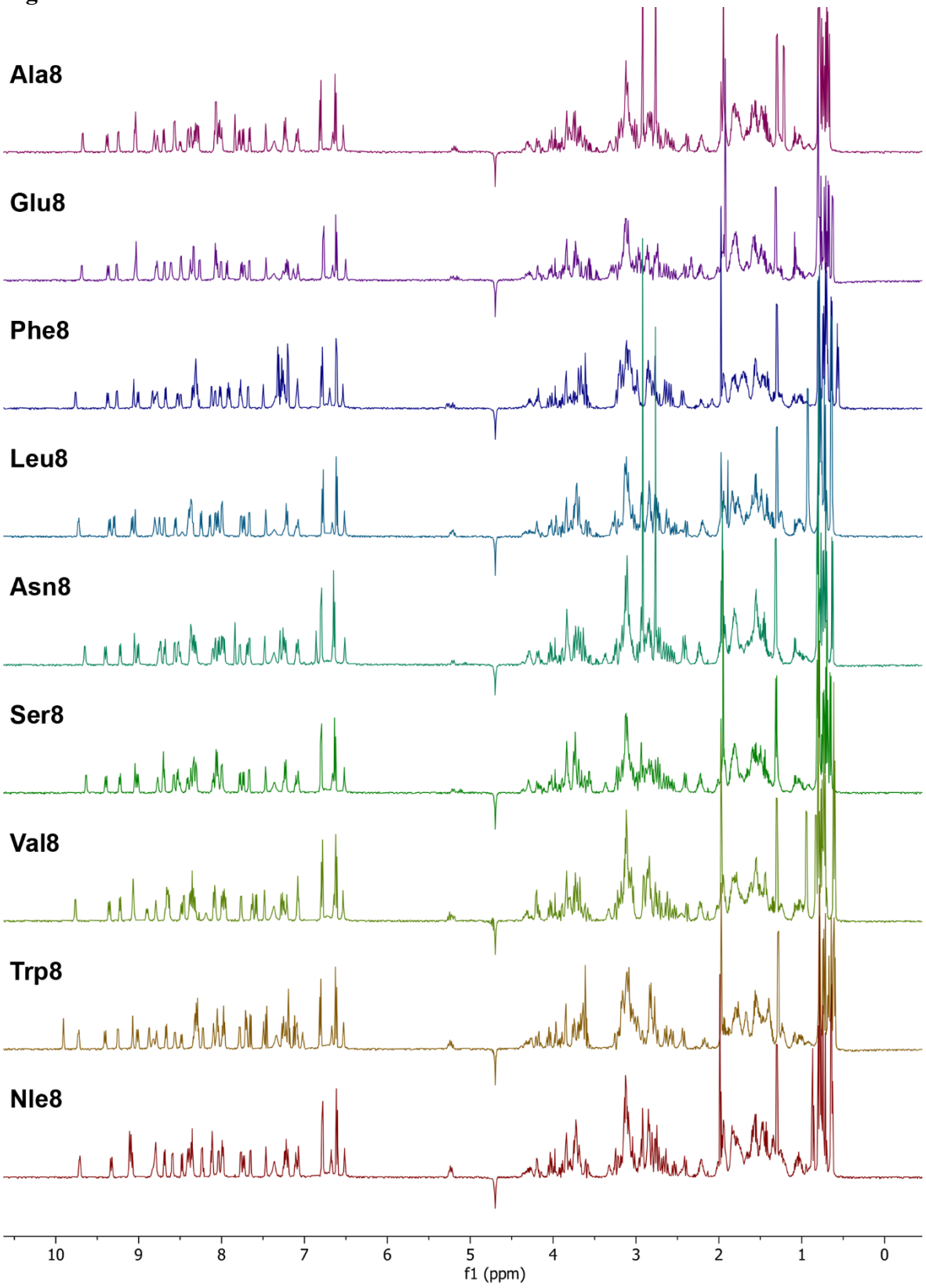

Figure S7. ^{1}H 1D NMR spectra for knottin variants with amino acid substitutions at P3′. Peptide sequences are listed in Table S3 (page S20).

Figure S8

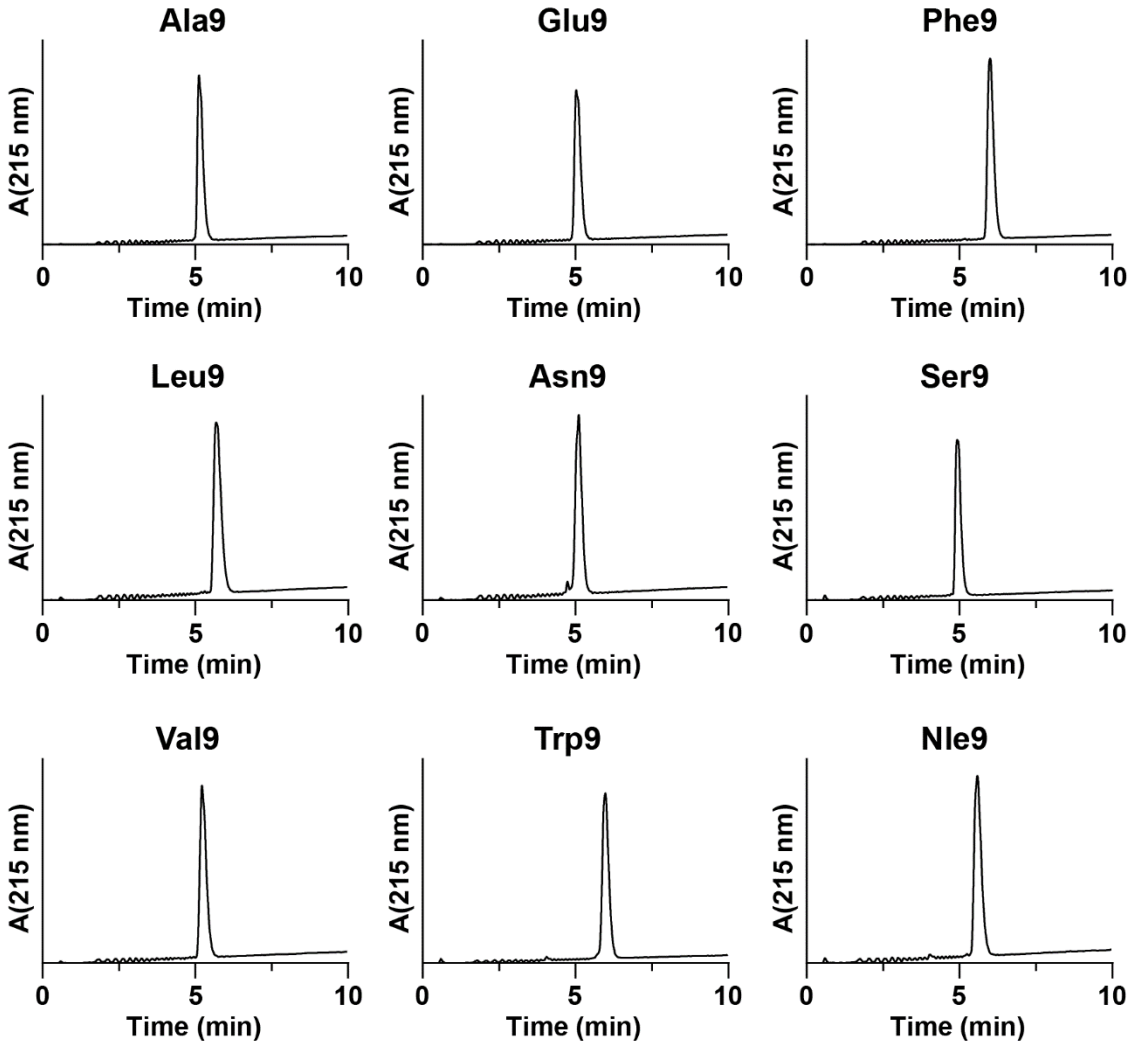

Figure S8. Analytical UHPLC traces for knottin variants with amino acid substitutions at P4′. Data were acquired using a Shimazdu Nexera UHPLC system equipped with a Phenomenex Luna Omega C18 column (1.6 µm 100 Å, 50 × 2.1 mm). Peptide sequences are listed in Table S4 (page S23). Nle denotes norleucine.

Table S4

Comp.	Sequence[a]	Theoretical $[M+3H]^{3+}$	Observed $[M+3H]^{3+}$	Purity (%)
Ala9	RVCPRILK**A**CRRDSDCPGACICRGNGYCG	1046.9	1046.8	>99
Glu9	RVCPRILK**E**CRRDSDCPGACICRGNGYCG	1066.2	1066.2	>99
Phe9	RVCPRILK**F**CRRDSDCPGACICRGNGYCG	1072.3	1072.2	>99
Leu9	RVCPRILK**L**CRRDSDCPGACICRGNGYCG	1060.9	1060.8	>99
Asn9	RVCPRILK**N**CRRDSDCPGACICRGNGYCG	1061.2	1061.2	97.8
Ser9	RVCPRILK**S**CRRDSDCPGACICRGNGYCG	1052.2	1051.8	>99
Val9	RVCPRILK**V**CRRDSDCPGACICRGNGYCG	1056.3	1056.2	>99
Trp9	RVCPRILK**W**CRRDSDCPGACICRGNGYCG	1085.3	1085.2	>99
Nle9	RVCPRILK**Nle**CRRDSDCPGACICRGNGYCG	1060.9	1060.9	>99

[a]Residue substitutions are shown in red bold font. Nle = norleucine

Figure S9

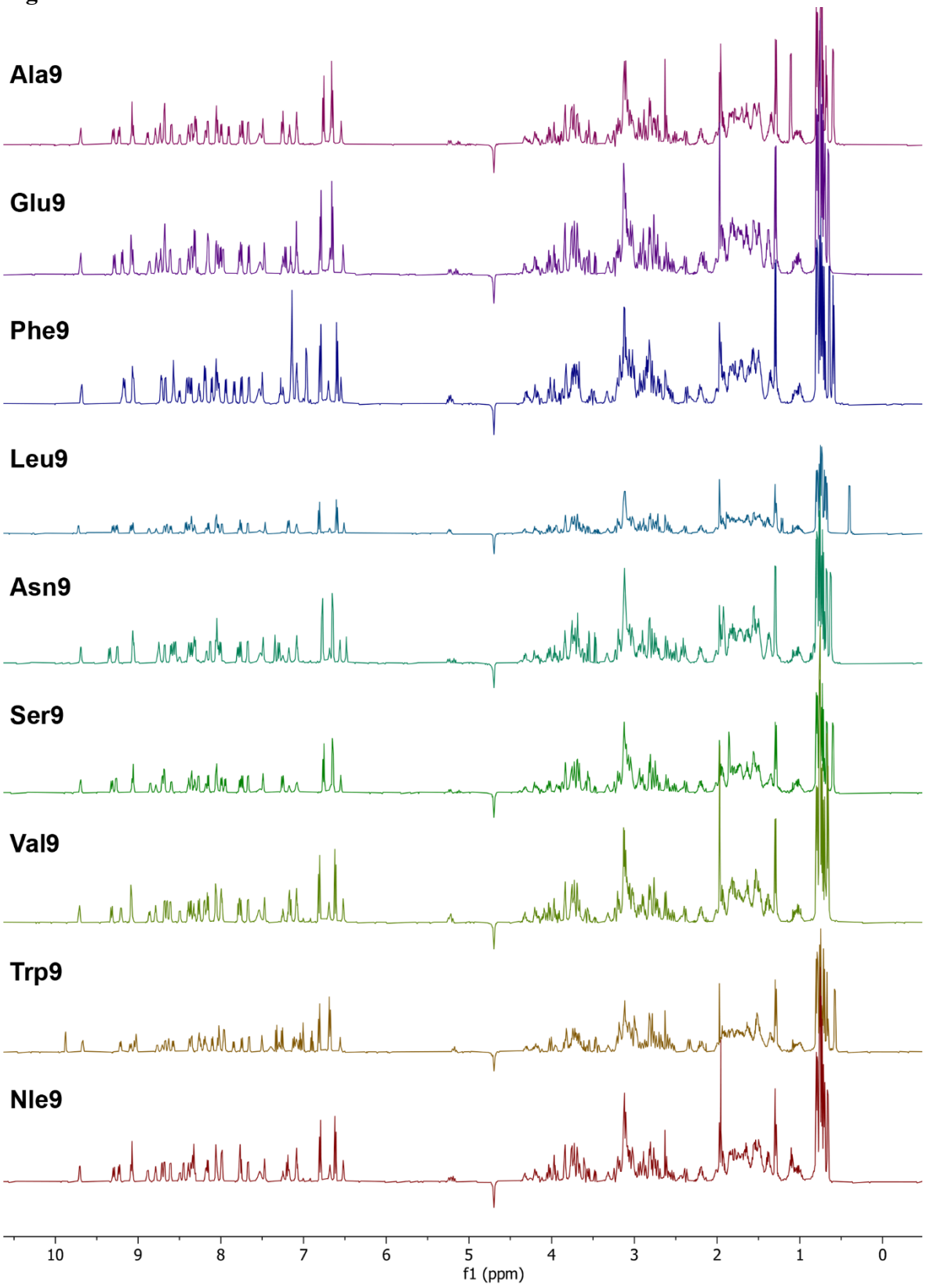

Figure S9. ^{1}H 1D NMR spectra for knottin variants with amino acid substitutions at P4′. Peptide sequences are listed in Table S4 (page S23).

Figure S10

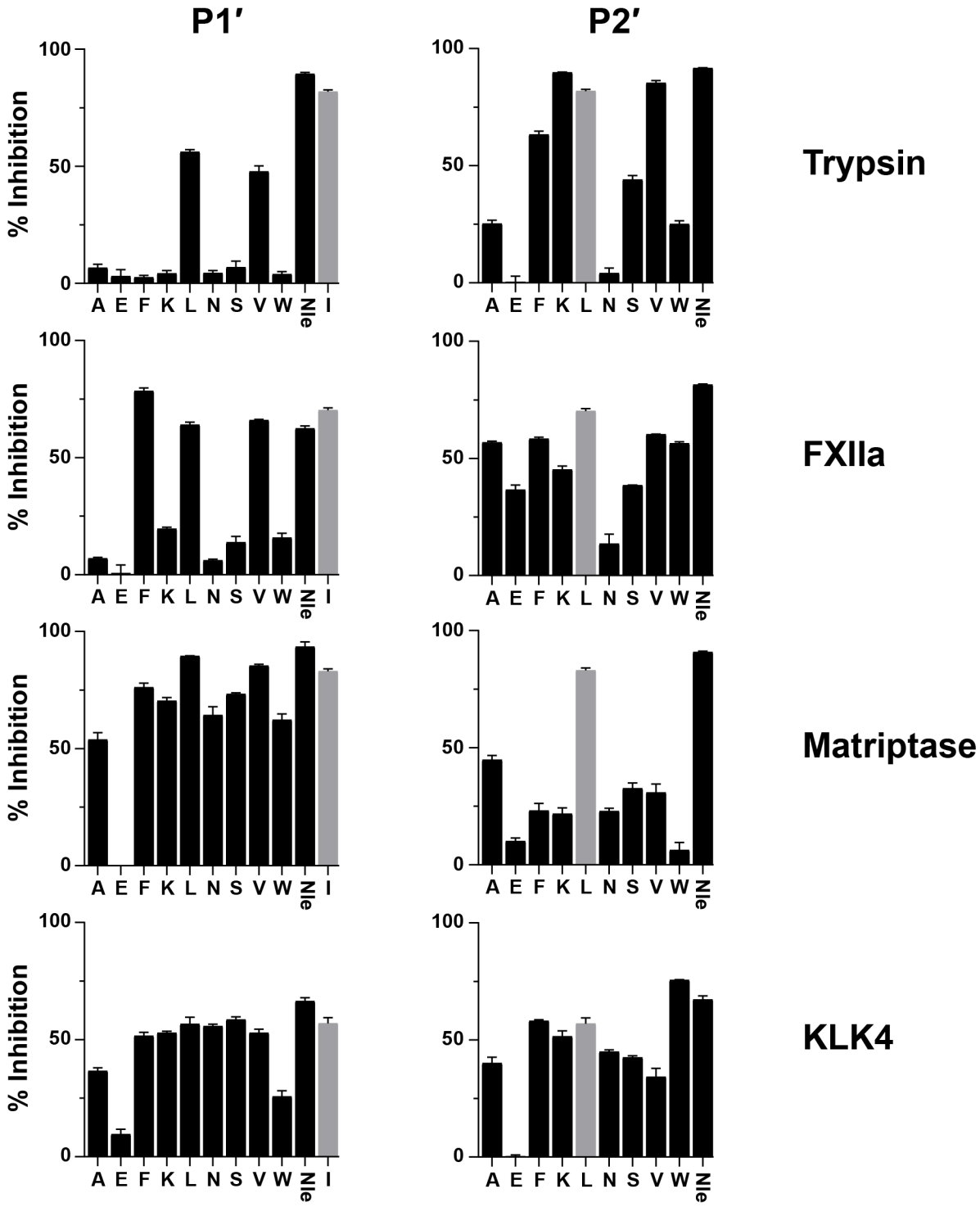
P1′
P2′
% Inhibition
100
50
0
A E F K L N S V W Nle I
Trypsin
FXIIa
Matriptase
KLK4

Figure S10 (continued)

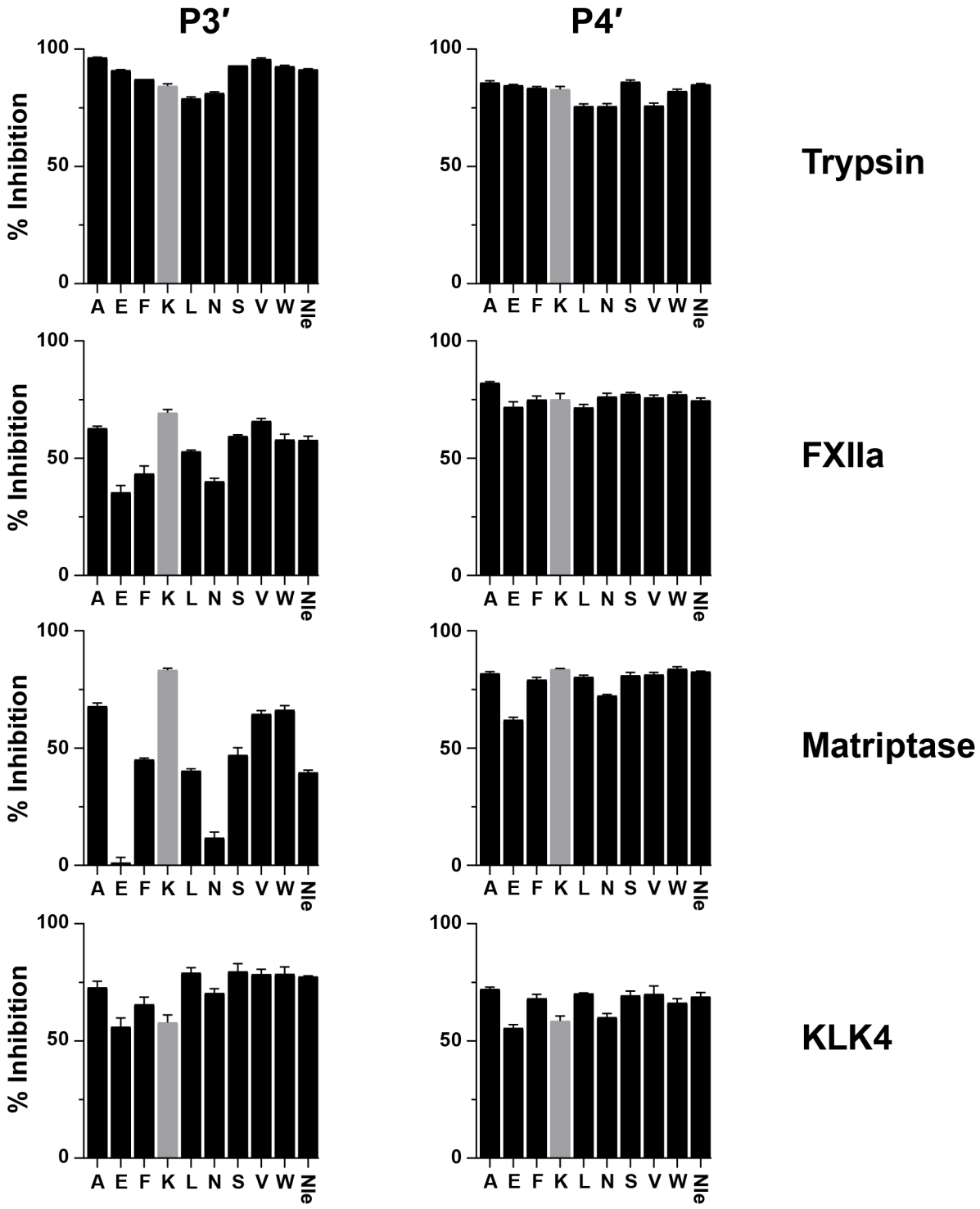

Figure S10. Specificity profiles for four serine proteases at the P1′–P4′ positions in a synthetic knottin PI. Bar graphs illustrate the inhibitory activity (% inhibition relative to control rates in the absence of inhibitor, *y*-axis) for individual knottin variants with various amino acids (*x*-axis) at a given position (indicated at the top of the figure). A fixed concentration of inhibitor was screened against each protease (trypsin: 10 nM, FXIIa: 25 nM, matriptase: 5 nM, KLK4: 1.25 nM). Inhibitory activity was calculated from three experiments performed in duplicate and is shown as the mean ± SD. Data were used to generate heat maps in Figure 1. Nle denotes norleucine.

Supplementary Results 2

Differences in the P1′–P2′ specificity of FXIIa compared to the other enzymes screened revealed several substitutions of interest. At P1′, Phe was the optimal residue for FXIIa but poorly favoured by trypsin, whereas at P2′, Glu was tolerated by FXIIa, but not by any of the other enzymes screened. To explore the chemical space around these hits, we synthesised additional variants with related proteinogenic or non-proteinogenic amino acids. For P1′ Phe, we tested modifications at the *para* position of the phenyl ring: Tyr, 4-fluoro-L-Phe, and 4-methyl-L-Phe. Both non-proteinogenic amino acids were slightly more preferred by FXIIa compared to Phe, but Tyr was poorly favoured (Figure S12). Each variant maintained weak activity against trypsin, whereas 4-methyl-L-Phe provided greater selectivity over KLK4 and 4-fluoro-L-Phe gave better selectivity over matriptase. For P2′ Glu, we varied the sidechain length using Asp or hGlu. Neither substitution was productive as Asp was poorly favoured by all four enzymes, and hGlu led to improved activity against matriptase but not FXIIa. We also compared P3′ Lys and Arg to select the optimal basic residue. P3′ Arg led to slightly improved activity against FXIIa, but also for matriptase and KLK4.

With the additional specificity data in hand, we synthesised a second peptide library to identify the optimal sequence combination for FXIIa. The P1′ residue was fixed as 4-fluoro-L-Phe, which was highly preferred by FXIIa but not trypsin or matriptase. At P2′, we selected residues that were preferred by FXIIa but not favoured by one or more off-targets (Trp and Val), as well as Glu as it was poorly favoured by all off-targets. Additionally, both P3′ residues (Lys and Arg) were included to account for any cooperativity effects with 4-fluoro-L-Phe at P1′. Inhibitor variants containing all possible combinations of these amino acids were produced by synthesising six peptides (**1**–**6**, Table S6). For comparison, we also included **MCoLib** and a variant with the most-preferred P1′–P4′ residues for FXIIa (**7**): 4-fluoro-L-Phe, Nle, Lys, Ala. The most potent FXIIa inhibitor was **7**, which showed a slight improvement in activity compared to **MCoLib** but limited selectivity over KLK4 and matriptase (Figure S14). Variants with P2′ Glu (**1** and **4**) showed the highest overall selectivity compared to inhibitors with P2′ Val (**2** and **5**) or Trp (**3** and **6**). Additionally, each inhibitor with P3′ Lys (**1**–**3**) outperformed the corresponding variant with P3′ Arg (**4**–**6**) for FXIIa, trypsin, and KLK4, but not matriptase.

Figure S11

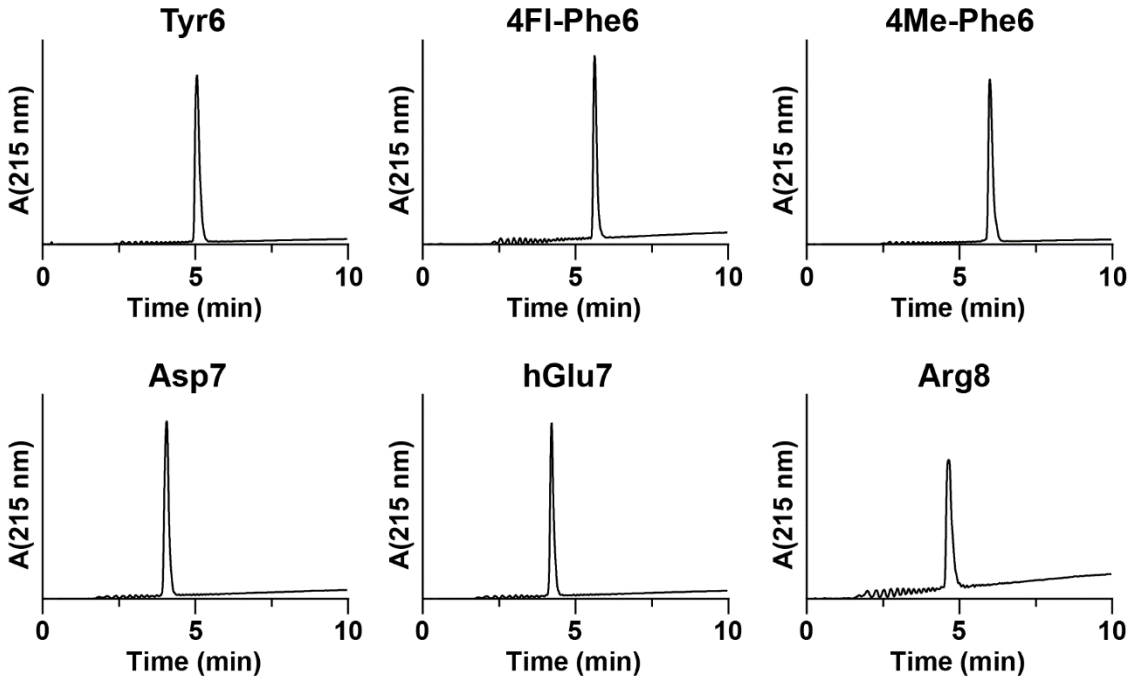

Figure S11. Analytical UHPLC traces for knottin variants with additional amino acid substitutions at P1′–P3′. Data were acquired using a Shimazdu Nexera UHPLC system equipped with a Phenomenex Luna Omega C18 column (1.6 µm 100 Å, 50 × 2.1 mm). Peptide sequences are listed in Table S5 (below).

Table S5

Comp.	Sequence[a]	Theoretical $[M+3H]^{3+}$	Observed $[M+3H]^{3+}$	Purity (%)
Tyr6	RVCPR**Y**LKKCRRDSDCPGACICRGNGYCG	1082.6	1082.4	>99
4Fl-Phe6	RVCPR**^{4F}F**LKKCRRDSDCPGACICRGNGYCG	1083.3	1083.1	>99
4Me-Phe6	RVCPR**^{4M}F**LKKCRRDSDCPGACICRGNGYCG	1081.9	1081.8	>99
Asp7	RVCPRI**D**KKCRRDSDCPGACICRGNGYCG	1066.6	1066.4	>99
hGlu7	RVCPRI**hE**KKCRRDSDCPGACICRGNGYCG	1075.9	1075.8	>99
Arg8	RVCPRIL**R**KCRRDSDCPGACICRGNGYCG	1075.3	1075.2	>99

[a]Residue substitutions are shown in red bold font. ^{4F}F = 4-fluoro-L-Phe, ^{4M}F = 4-methyl-L-Phe, hE = L-homoGlu

Figure S12

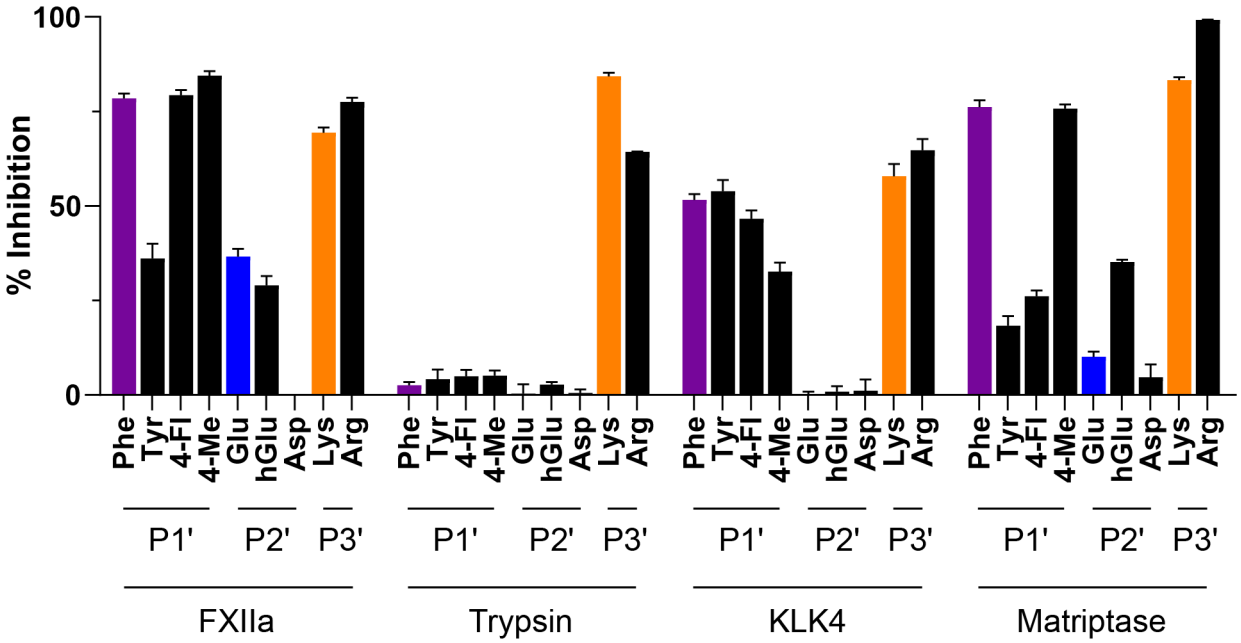

Figure S12. Inhibitory activity of knottin variants with additional amino acid substitutions at P1′–P3′. Amino acid substitutions are indicated on the *x*-axis (4-Fl = 4-fluoro-L-Phe, 4-Me = 4-methyl-L-Phe, hGlu = L-homoGlu), with the initial residue from the knottin library highlighted with a coloured bar (purple: P1′, blue: P2′, orange: P3′). A fixed concentration of inhibitor was screened against each protease (FXIIa: 25 nM, trypsin: 10 nM, KLK4: 1.25 nM, matriptase: 5 nM). Peptide sequences are listed in Table S5 (page S28) and data represent the mean ± SD from three experiments performed in duplicate.

Figure S13

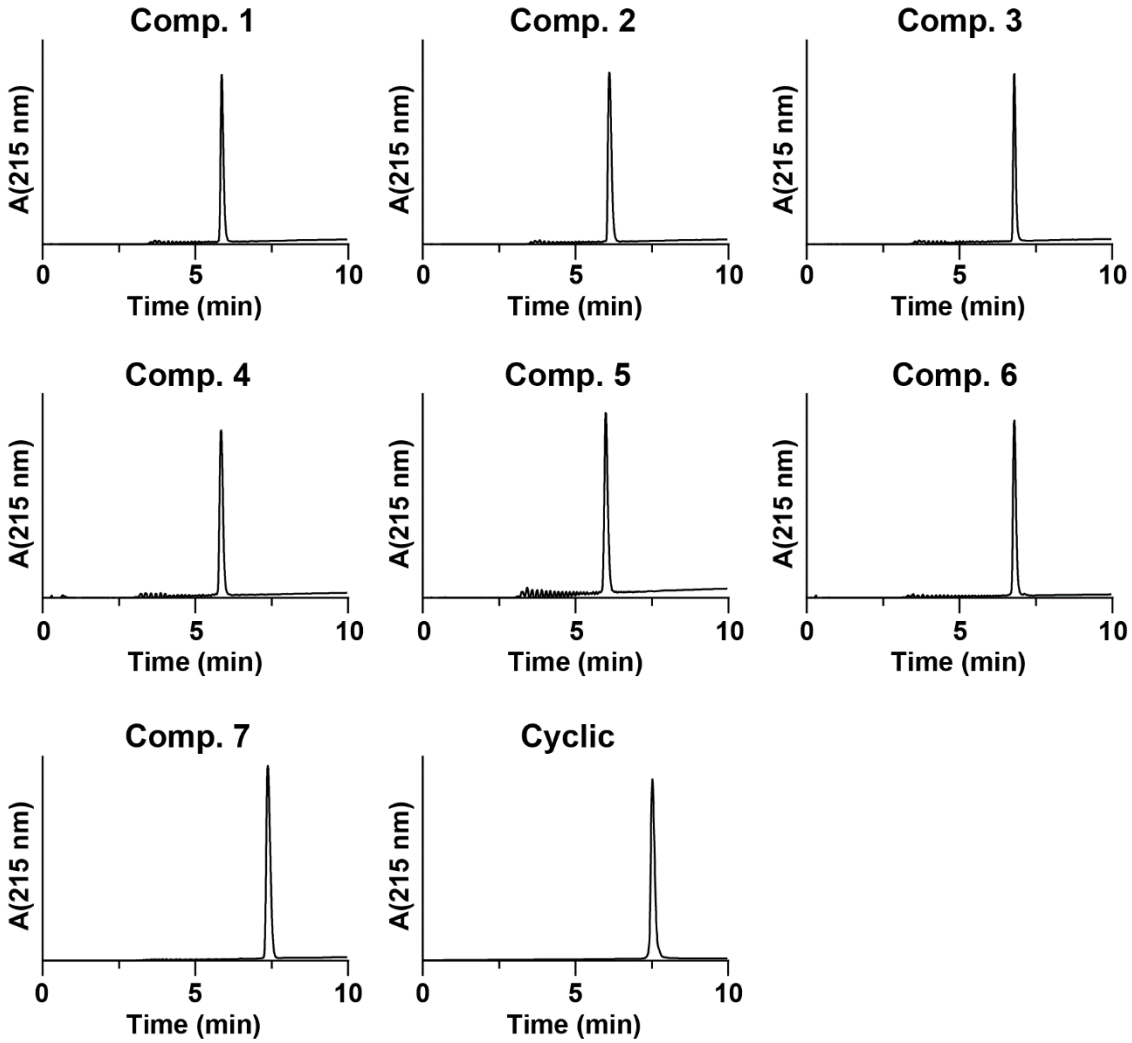

Figure S13. Analytical UHPLC traces for a focused library of knottin variants. Data were acquired using a Shimazdu Nexera UHPLC system equipped with a Phenomenex Luna Omega C18 column (1.6 µm 100 Å, 50 × 2.1 mm). Peptide sequences are listed in Table S6 (page S31).

Table S6

Comp.	Sequence[a]	Theoretical $[M+3H]^{3+}$	Observed $[M+3H]^{3+}$	Purity (%)
1	RVCPR^{4F}**FE**KKCRRDSDCPGACICRGNGYCG	1088.6	1088.5	>99
2	RVCPR^{4F}**FV**KKCRRDSDCPGACICRGNGYCG	1078.6	1078.5	>99
3	RVCPR^{4F}**FW**KKCRRDSDCPGACICRGNGYCG	1107.6	1107.5	>99
4	RVCPR^{4F}**FER**KCRRDSDCPGACICRGNGYCG	1097.9	1097.8	>99
5	RVCPR^{4F}**FVR**KCRRDSDCPGACICRGNGYCG	1087.9	1087.8	>99
6	RVCPR^{4F}**FWR**KCRRDSDCPGACICRGNGYCG	1117.0	1116.9	>99
7	RVCPR^{4F}**FNle**K**A**CRRDSDCPGACICRGNGYCG	1064.3	1164.1	>99
Cyclic	GGVCPR^{4F}**FE**KKCRRDSDCPGACICRGNGYCGSGSD	1184.0	1183.8	>99

[a]Residue substitutions are shown in red bold font ('cyclic' has a backbone amide bond between Gly1–Asp34). Nle = norleucine, ^{4F}F = 4-fluoro-L-Phe.

Figure S14

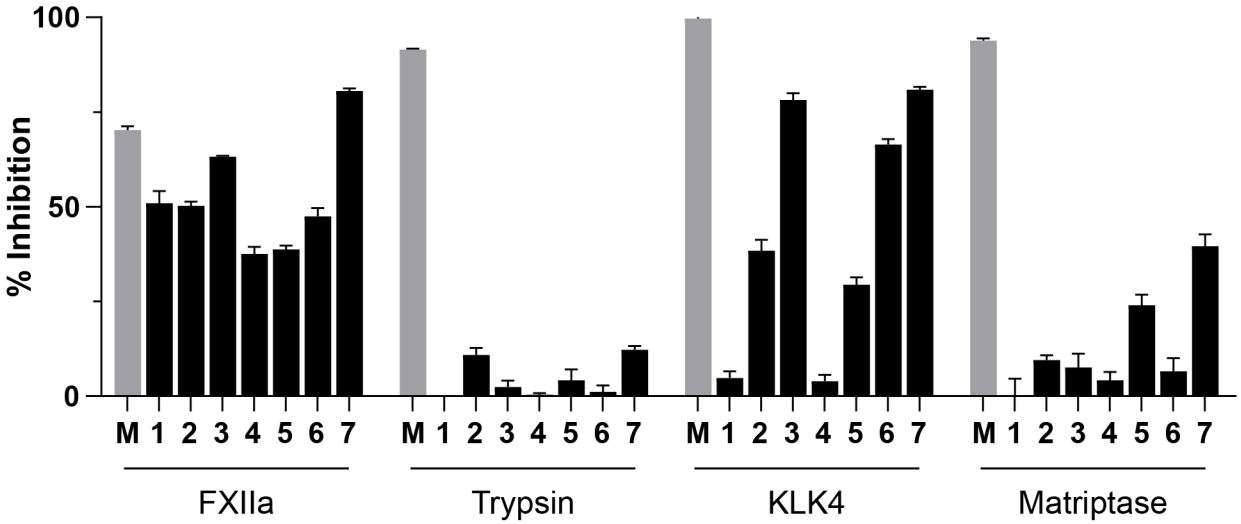

Figure S14. Inhibitory activity of a focused library of knottin variants with additional amino acid substitutions at P1′–P3′. Inhibitors were screened at a fixed concentration of 25 nM against each protease. On the *x*-axis, **M** denotes the parent molecule **MCoLib** (grey bar) and peptide sequences for **1**–**7** are listed in Table S6 (page S31). Data represent the mean ± SD from three experiments performed in duplicate.

Figure S15

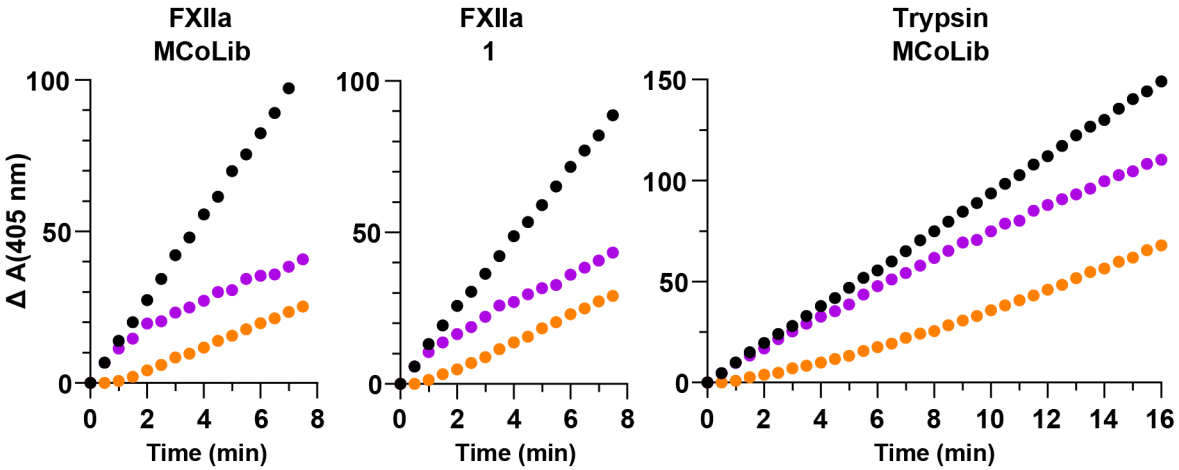

Figure S15. Reaction progress curves showing enzyme activity (*y*-axis, mOD) after addition of substrate to FXIIa or trypsin pre-incubated with inhibitor (orange) or simultaneously with inhibitor (purple). Enzyme activity in the absence of inhibitor (black) illustrates the control rate. Progress curves were used to calculate k_{off} for each enzyme–inhibitor pair using the method described by Baici and Gyger-Marazzi.[7] For these calculations, values on the *x*-axis were plotted in seconds.

Table S7

Selectivity analysis for compound 1

Protease[a]	K_i (nM)
FXIIa	11 ± 0.8
Trypsin	2940 ± 85
Matriptase	2830 ± 130
KLK4	IC_{50} > 10,000 (29% inhibition)
Thrombin	IC_{50} > 10,000 (5% inhibition)
FXa	IC_{50} > 10,000 (0% inhibition)
FXIa	IC_{50} > 10,000 (17% inhibition)
Plasmin	IC_{50} > 10,000 (16% inhibition)
Plasma kallikrein	IC_{50} > 10,000 (3% inhibition)
uPA	IC_{50} > 10,000 (0% inhibition)
tPA	IC_{50} > 10,000 (6% inhibition)

[a]tPA = tissue-type plasminogen activator, uPA = urokinase-type plasminogen activator

Figure S16

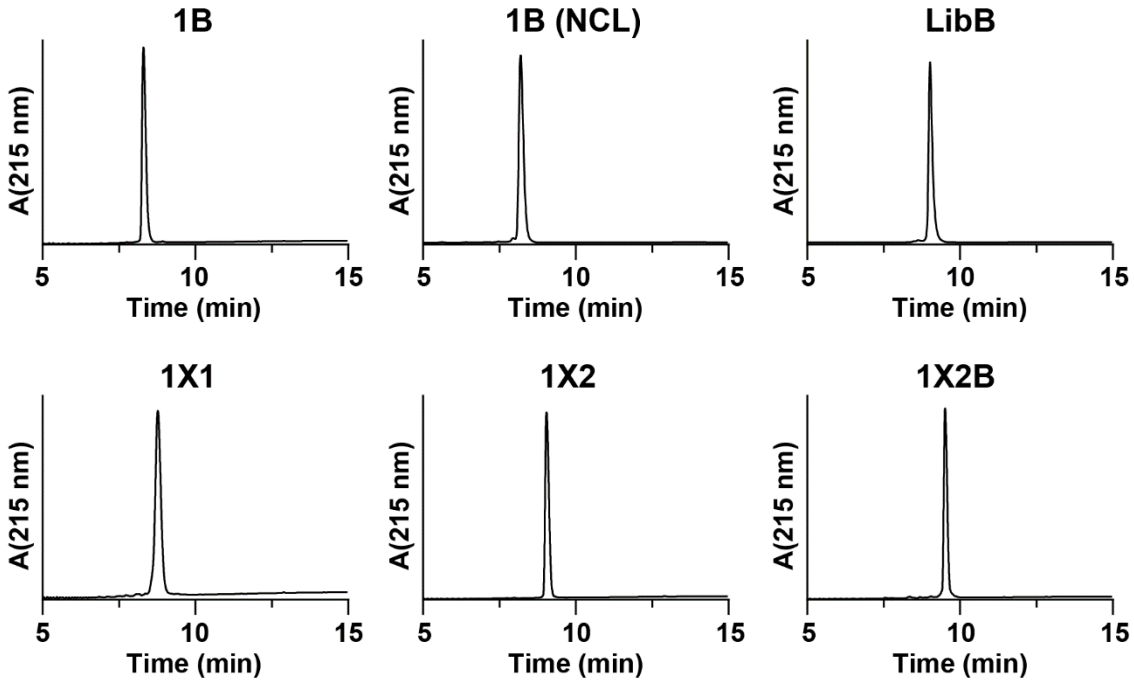

Figure S16. Analytical HPLC traces for functionalised knottin variants. Data were acquired using a Shimadzu Nexera XR system equipped with a Phenomenex Jupiter C18 column (5 µm 300 Å, 150 × 2 mm). Peptide sequences are listed in Table S8 (below).

Table S8

Comp.	Sequence[a]	Theoretical $[M+3H]^{3+}$	Observed $[M+3H]^{3+}$	Purity (%)
1X1	RVCPR**^{4F}FE**K**X**CRRDSDCPGACICRGNGYCG	1108.6	1108.4	98.6
1X2	**X**RVCPR**^{4F}FE**KK**C**RRDSDCPGACICRGNGYCG	1151.3	1151.2	>99
1B	RVCPR**^{4F}FE**K**B**CRRDSDCPGACICRGNGYCG	1164.0	1164.0	>99
1B (NCL)	RVCPR**^{4F}FE**K**B**CRRDSDCPGACICRGNGYCG	1164.0	1163.9	97.4
LibB	RVCPRILK**B**CRRDSDCPGACICRGNGYCG	1143.4	1141.3	98.2
1X2B	**X**RVCPR**^{4F}FE**K**B**CRRDSDCPGACICRGNGYCG	1226.8	1226.6	>99

[a]Residue substitutions are shown in red bold font. ^{4F}F = 4-fluoro-L-Phe, X = 4-azido-L-Phe, B = Nε-biotinyl-L-Lys

Figure S17

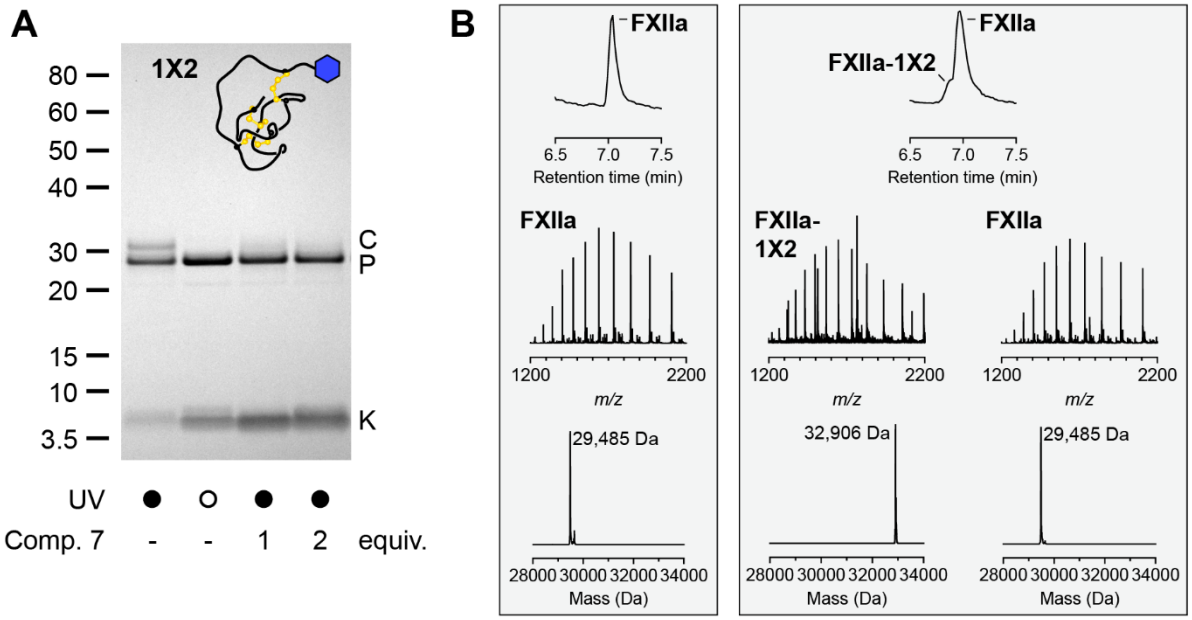

Figure S17. A) SDS-PAGE analysis showing additional controls for **1X2**, where FXIIa and **1X2** were not exposed to UV light (lane 2), or FXIIa was pre-incubated with a high-affinity competing inhibitor (compound **7**, Table S6) prior to adding **1X2** and exposing to UV light (lanes 3–4). For comparison, **1X2** crosslinked to FXIIa is also shown (lane 1). B) Reconstructed ESI-MS spectra for FXIIa only (left panel) or the products of a crosslinking reaction with FXIIa and **1X2** (right panels). The calculated shift in mass from FXIIa only (29,485 Da) for the crosslinked complex (32,906 Da) was 3,421 Da, which corresponds to the mass of **1X2** (3,448.5 Da) minus two nitrogen atoms that are lost upon photoactivation.

Figure S18

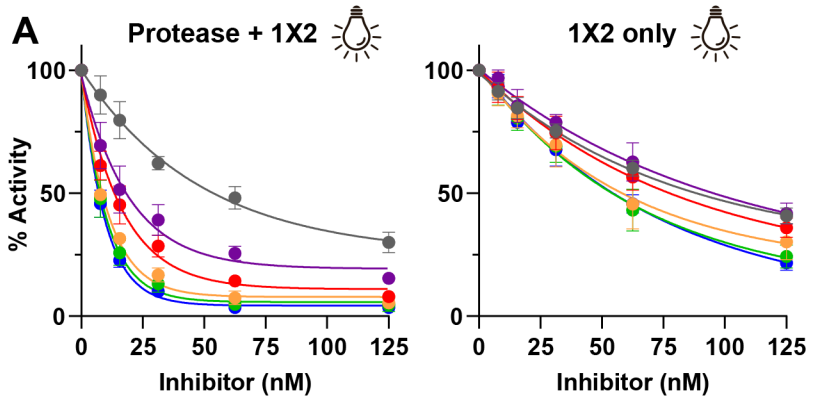

FXIIa IC_{50} (nM)	P + 1X2	1X2 only
No UV	54 ± 5	88 ± 5
30 s	18 ± 2	95 ± 7
1 min	13 ± 1	76 ± 6
2 min	8 ± 0.4	58 ± 6
3 min	8 ± 0.5	54 ± 5
5 min	7 ± 0.3	54 ± 3

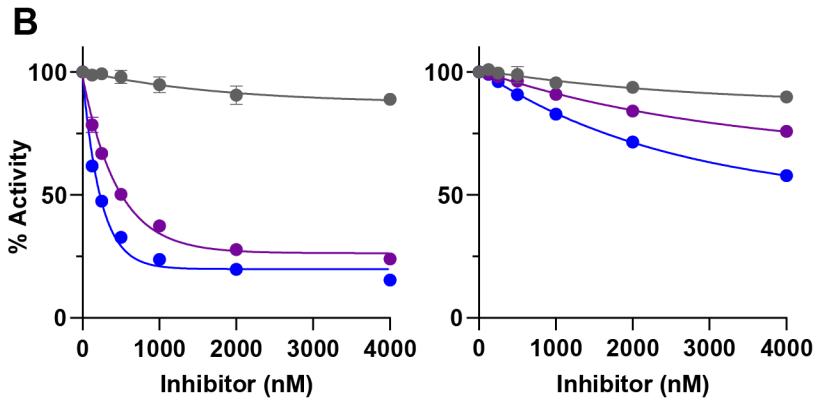

Trypsin IC_{50} (nM)	P + 1X2	1X2 only
No UV	> 10 μM	> 10 μM
30 s	510 ± 20	> 4 μM
1 min	N.D.	N.D.
2 min	N.D.	N.D.
3 min	N.D.	N.D.
5 min	220 ± 10	> 4 μM

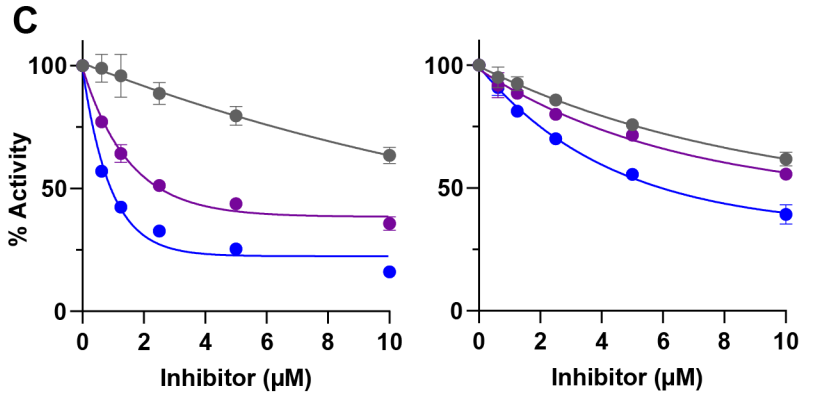

KLK4 IC_{50} (μM)	P + 1X2	1X2 only
No UV	> 10 μM	> 10 μM
30 s	2.5 ± 0.2	> 10 μM
1 min	N.D.	N.D.
2 min	N.D.	N.D.
3 min	N.D.	N.D.
5 min	0.9 ± 0.07	5.9 ± 0.3

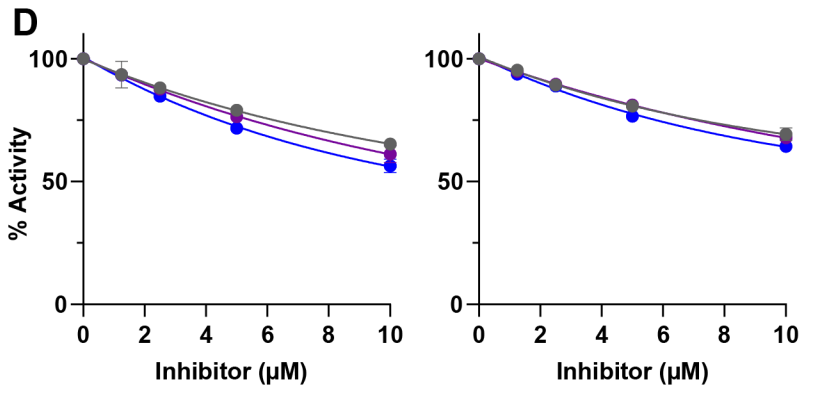

Matriptase IC_{50} (μM)	P + 1X2	1X2 only
No UV	> 10 μM	> 10 μM
30 s	> 10 μM	> 10 μM
1 min	N.D.	N.D.
2 min	N.D.	N.D.
3 min	N.D.	N.D.
5 min	> 10 μM	> 10 μM

Figure S18. A photoreactive knottin with light-controlled selectivity. Graphs show data (mean ± SD) from competitive inhibition assays comparing the activity of **1X2** against A) FXIIa, B) trypsin, C) KLK4 or D)

matriptase with varying UV exposure times. Left panels show data for exposure of protease and **1X2** to UV light (exposure times are indicated in the key below the last graph). Data for each exposure time are normalised to controls (protease without inhibitor) exposed to UV light for the same time. Right panels show data for exposure of **1X2** only prior to incubating with protease. IC_{50} values calculated for each exposure time are shown in the tables on the far right. For trypsin, KLK4 and matriptase, exposure times of 1–3 min were not performed (N.D. = not determined). Data represent the mean ± standard error from three experiments performed in duplicate.

Figure S19

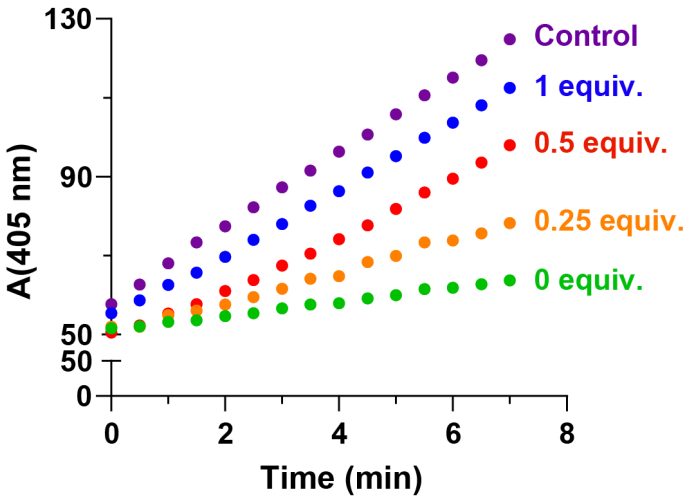

Figure S19. Progress curves for FXIIa activity after adding substrate immediately after streptavidin. FXIIa (12 nM) was incubated with **1B** (250 nM) for 10 min (100 µL – final concentrations were FXIIa: 6 nM, **1B**: 125 nM). Varying concentrations of streptavidin (0 – 1 equiv.) were then added, followed immediately by substrate (120 µM). Activity was monitored at λ = 405 nm (*y*-axis, mOD). Control (purple) indicates substrate added to FXIIa without inhibitor. Data are representative of one out of three experiments performed in triplicate.

Supplementary Results 3

To further explore the use of streptavidin for modulating the activity of biotinylated knottins, we examined whether a biotin tag could be added to **1X2** to generate a labelled knottin (**1X2B**) that has light-controlled activity. In assays performed before crosslinking, **1X2B** inhibits FXIIa (IC_{50} = 128 nM) but has poor activity against trypsin (17% inhibition at 10 μM). After crosslinking, we observed improved activity against FXIIa and trypsin, with apparent IC_{50} values of 11 nM and 280 nM, respectively, after 5 min UV exposure (Figure S20A). These levels of activity are similar to non-labelled **1X2** (Figure S18). We also tested the effect of adding streptavidin, anticipating that the recovery of activity would be lower after crosslinking the inhibitor and enzyme. For FXIIa, adding streptavidin led to a small recovery in activity (Figure S20B). These data reflect that non-crosslinked **1X2B** is an effective, but reversible FXIIa inhibitor (non-crosslinked FXIIa and **1X2B** remain present after UV exposure, as shown in Figure 3). Accordingly, adding streptavidin allows the effect of inhibition by remaining non-crosslinked **1X2B** to be separated from crosslinking of **1X2B** and FXIIa. By contrast, no recovery of trypsin activity was observed after streptavidin addition as non-crosslinked **1X2B** is a weak trypsin inhibitor, further supporting that the improvement in trypsin inhibition can be attributed to crosslinking.

Figure S20

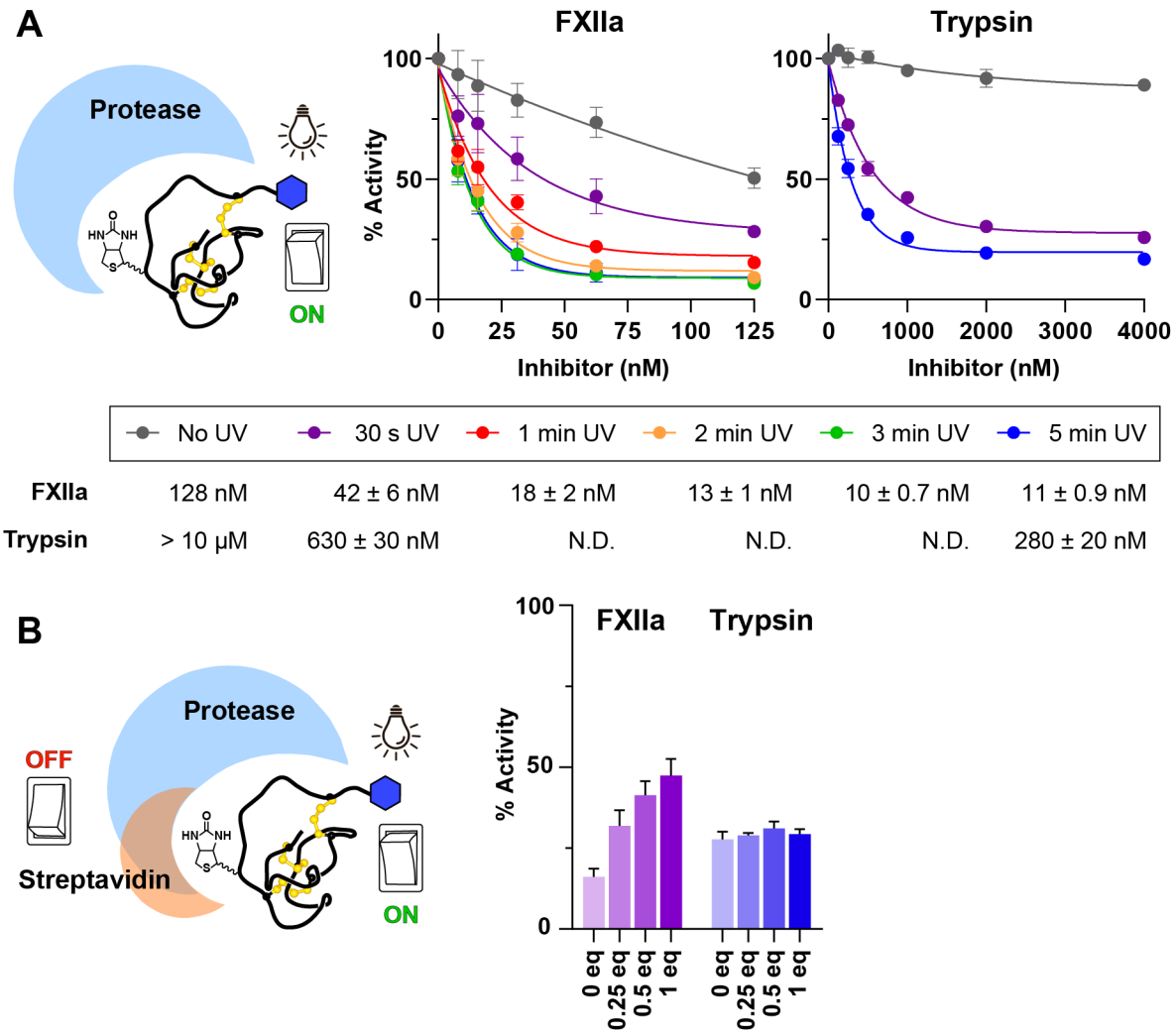

Figure S20. A) Graphs show data (mean ± SD, three experiments) from competitive inhibition assays comparing the activity of **1X2B** against FXIIa or trypsin with or without exposure to UV light. Exposure times are indicated in the key below the graphs. Data for each exposure time are normalised to controls (protease without inhibitor) exposed to UV light for the same time. IC_{50} values calculated for each exposure time are shown below the key. B) Effect of adding 0–1 equiv. streptavidin (*x*-axis) on the activity of FXIIa or trypsin after crosslinking with **1X2B**. Crosslinking was performed using 48 nM FXIIa and 500 nM **1X2B** (3 min UV exposure), or 0.8 nM trypsin and 8 µM **1X2B** (5 min UV exposure) – this material was diluted 1/8 to perform activity assays (final concentrations: 6 nM FXIIa and 62.5 nM **1X2B**, or 0.1 nM trypsin and 1 µM **1X2B**). Final assay concentrations of **1X2B** were used to calculate streptavidin equiv. to be added. Activity data are expressed as a % relative to controls with protease and substrate only (mean ± SD from three experiments).

Figure S21

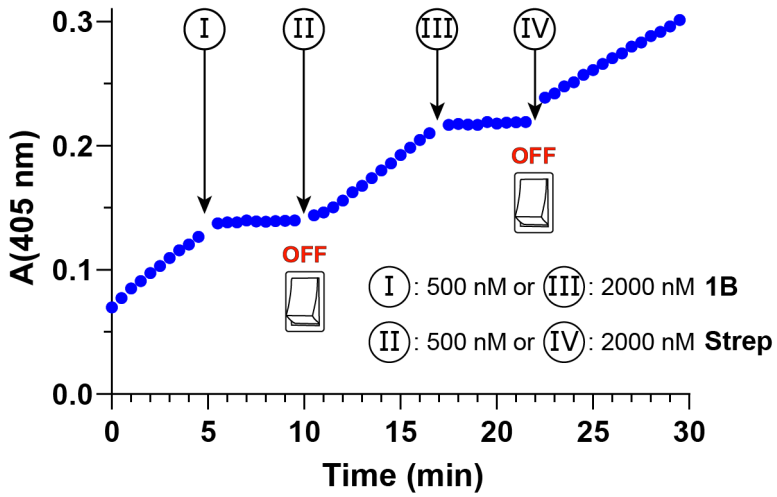

Figure S21. Streptavidin rapidly switches OFF a biotin-labelled knottin. The progress curve shows substrate cleavage by FXIIa (*y*-axis, OD). Reactions were initiated by adding FXIIa (5 nM) to substrate (150 µM). At 5 min (I), **1B** (500 nM) was added to stop the reaction. At 10 min (II), streptavidin (500 nM) was added. Recovery of FXIIa activity after adding streptavidin exceeded 90% relative to the control rate. At 17 min (III), **1B** (2000 nM) was added to stop the reaction. At 22 min (IV), streptavidin (2000 nM) was added. Recovery of FXIIa activity was ~70% relative to the control rate. Data show a representative curve from one of three experiments performed in triplicate.

References

[1] S. J. de Veer, J. E. Swedberg, M. Akcan, K. J. Rosengren, M. Brattsand, D. J. Craik, J. M. Harris, *Biochem. J.* **2015**, *469*, 243-253.

[2] C. Y. Li, S. J. de Veer, R. H. P. Law, J. C. Whisstock, D. J. Craik, J. E. Swedberg, *ChemBioChem* **2019**, *20*, 46-50.

[3] J. Du, K. Yap, L. Y. Chan, F. B. H. Rehm, F. Y. Looi, A. G. Poth, E. K. Gilding, Q. Kaas, T. Durek, D. J. Craik, *Nat. Commun.* **2020**, *11*, 1575.

[4] K. Yap, J. Du, F. B. H. Rehm, S. R. Tang, Y. Zhou, J. Xie, C. K. Wang, S. J. de Veer, L. H. L. Lua, T. Durek, D. J. Craik, *Nat. Protoc.* **2021**, *16*, 1740-1760.

[5] G. M. Fang, Y. M. Li, F. Shen, Y. C. Huang, J. B. Li, Y. Lin, H. K. Cui, L. Liu, *Angew. Chem. Int. Ed.* **2011**, *50*, 7645-7649.

[6] D. T. Flood, J. C. J. Hintzen, M. J. Bird, P. A. Cistrone, J. S. Chen, P. E. Dawson, *Angew. Chem. Int. Ed.* **2018**, *57*, 11634-11639.

[7] A. Baici, M. Gyger-Marazzi, *Eur. J. Biochem.* **1982**, *129*, 33-41.

[8] C. N. Zdenek, C. Hay, K. Arbuckle, T. N. W. Jackson, M. H. A. Bos, B. Op den Brouw, J. Debono, L. Allen, N. Dunstan, T. Morley, M. Herrera, J. M. Gutierrez, D. J. Williams, B. G. Fry, *Toxicol. In Vitro* **2019**, *58*, 97-109.

[9] W. Liu, S. J. de Veer, Y. H. Huang, T. Sengoku, C. Okada, K. Ogata, C. N. Zdenek, B. G. Fry, J. E. Swedberg, T. Passioura, D. J. Craik, H. Suga, *J. Am. Chem. Soc.* **2021**, *143*, 18481-18489.

[10] J. S. Mylne, L. Y. Chan, A. H. Chanson, N. L. Daly, H. Schaefer, T. L. Bailey, P. Nguyencong, L. Cascales, D. J. Craik, *Plant Cell* **2012**, *24*, 2765-2778.

[11] J. Kowalska, A. Zablocka, T. Wilusz, *Biochim. Biophys. Acta* **2006**, *1760*, 1054-1063.

[12] W. Bode, H. J. Greyling, R. Huber, J. Otlewski, T. Wilusz, *FEBS Lett.* **1989**, *242*, 285-292.

[13] Q. Huang, S. Liu, Y. Tang, *J. Mol. Biol.* **1993**, *229*, 1022-1036.

[14] D. S. Wishart, C. G. Bigam, A. Holm, R. S. Hodges, B. D. Sykes, *J. Biomol. NMR* **1995**, *5*, 67-81.